

Discrete transparent boundary conditions for the equation of rod transverse vibrations

Vladimir A. Gordin^{a,b}, Aleksandr A. Shemendyuk^{a,*}

^a National Research University Higher School of Economics, Moscow, Russia

^b Hydrometeorological Centre of Russia, Moscow 123242, Russia

ARTICLE INFO

Article history:

Received 3 March 2019

Revised 18 June 2020

Accepted 28 June 2020

Available online 7 July 2020

Keywords:

Rod equation

Boundary condition

Rational approximation

Finite-difference approximation

Implicit scheme

Z-Transformation

ABSTRACT

Local perturbations of an infinitely long rod travel to infinity. On the contrary, in the case of a finite length of the rod, the perturbations reach its boundary and are reflected. The boundary conditions constructed here for the implicit difference scheme imitate the Cauchy problem and provide almost no reflection. These boundary conditions are non-local with respect to time, and their practical implementation requires additional calculations at every time step. To minimise them, a special rational approximation, similar to the Hermite - Padé approximation is used. Numerical experiments confirm the high “transparency” of these boundary conditions and determine the conditional stability regions for finite-difference scheme.

© 2020 Elsevier Inc. All rights reserved.

1. Introduction

The equation of transverse vibrations of a rod (beam) with a circular cross section

$$\rho \frac{\partial^2 u}{\partial t^2} - \frac{\partial}{\partial x} \left[R^2 \rho \frac{\partial^3 u}{\partial x \partial t^2} \right] + \frac{\partial^2}{\partial x^2} \left[ER^2 \frac{\partial^2 u}{\partial x^2} \right] = f \quad (1)$$

has many applications, see e.g. [1]. Here $x \in [-L/2, L/2]$ is the spatial variable, L is the length of the rod, t is time, ρ is the density of the rod, R is the radius of the cross section of the rod, E is the Young's modulus of the rod, the unknown function $u = u(t, x)$ describes the transverse displacement of the rod. The right hand side (forcing) f describes external force.

The kinetic energy of transverse vibrations of a rod is defined as

$$\mathbf{K}[u] = \frac{1}{2} \int_{-L/2}^{L/2} \rho \left[\left(\frac{\partial u}{\partial t} \right)^2 + R^2 \left(\frac{\partial^2 u}{\partial t \partial x} \right)^2 \right] dx, \quad (2)$$

and its potential energy is

$$\mathbf{P}[u] = \frac{1}{2} \int_{-L/2}^{L/2} ER^2 \left(\frac{\partial^2 u}{\partial x^2} \right)^2 dx. \quad (3)$$

* Corresponding author at: National Research University Higher School of Economics, Moscow, Russia.

E-mail addresses: vagordin@mail.ru (V.A. Gordin), aashemendyuk@edu.hse.ru (A.A. Shemendyuk).

Eq. (1) could be obtained from the least action variation principle with Lagrangian $\mathcal{L} = \mathbf{K} - \mathbf{P}$. The Hamiltonian (energy) for Eq. (1) is then

$$\mathcal{H} = \mathbf{K} + \mathbf{P}. \quad (4)$$

The Cauchy problem for Eq. (1):

$$u(0, x) = U_0(x), \quad \partial_t u(0, x) = U_1(x), \quad x \in \mathbb{R},$$

is correct according to Hadamard. Two boundary conditions at each edge of the segment $x = \pm L/2$ provide the mixed initial-boundary value problem, if the corresponding boundary operators satisfy the Shapiro – Lopatinsky conditions (see [2–7]).

Let us assume that the forcing in Eq. (1) is absent: $f \equiv 0$. The energy \mathcal{H} remains unchanged for the Cauchy problem for Eq. (1). If, in the Cauchy problem, the support of initial value functions belongs to the segment

$$\text{supp } U_0 \subseteq [-L/2, L/2], \quad \text{supp } U_1 \subseteq [-L/2, L/2],$$

then for any time t the following inequality holds:

$$\mathbf{P}[u(t, x)] \leq \mathcal{H}[u(t, x)] \leq \frac{1}{2} \int_{-\infty}^{\infty} \left[\rho(U_1)^2 + \rho R^2 \left(\frac{\partial U_1}{\partial x} \right)^2 + ER^2 \left(\frac{\partial^2 U_0}{\partial x^2} \right)^2 \right] dx, \quad (5)$$

because the sub-integral expression is always non-negative. In numerical approximations of Eq. (1) the first integral \mathcal{H} can change with time due to rough discretization or because of boundary conditions.

The construction of boundary conditions that have no reflection of outgoing waves from the boundary for an implicit finite-difference equation (see Section 3), which approximates Eq. (1), is the subject of this article. There are various names of such boundary conditions (see Section 2). We use the name DTBCs (Discrete Transparent Boundary Conditions). We emphasise that for each finite-difference scheme it is necessary to construct “individual” DTBCs.

The construction is practically important, because of the place of this equation in the theory of elasticity and in engineering problems. The algorithm of the construction is technically more consuming than in the case of classical equations and systems of mathematical physics in partial derivatives considered earlier in [8–17], since (a) Eq. (1) is not resolved with respect to the highest (second) derivative with respect to time (i.e. it is not a differential equation of the Cauchy – Kovalevskaya type) and (b) the equation’s order with respect to the spatial variable is equal to 4.

The high order of the differential (and, as a consequence, of the finite-difference) equation with respect to space requires two boundary conditions at each edge. The DTBCs and Approximate DTBC (or simply ADTBCs) for various simpler finite-difference schemes approximating equations of mathematical physics were considered by authors earlier in [14,16,18–22].

The various versions of the TBCs, DTBCs, and ADTBCs may be developed for various equations and systems of the elasticity theory and their various discretizations, and such ADTBCs give the possibility of avoiding significant errors as a result of a false reflection from the boundary, when we solve local problems in a large area.

We introduce the absolutely stable finite-difference scheme that approximates the Cauchy problem for Eq. (1) with constant coefficients in Section 3. The construction of the DTBCs and ADTBCs for the finite-difference scheme will be considered in Section 4.3.

On the contrary, the implicit finite-difference scheme that approximates the mixed boundary value problem for Eq. (1) is not absolutely stable with our proposed ADTBCs. Stability conditions significantly differ from similar conditions for schemes that approximate the classical equations of mathematical physics (transport, diffusion, wave, Schrödinger, etc.). For them, usually, the stability condition is that the time step τ must not exceed some critical value. According to our numerical experiments, for the considered mixed problem with given boundary conditions the step τ must satisfy two inequalities at once. It appears that on the $\tau - h$ plane the range of values, at which stability takes place lies between two parabolas, see Section 4.5.

The description of the results of numerical experiments with ADTBCs, and comparisons with other boundary conditions, are in Section 5.

2. Transparent boundary condition problem overview

In many practical problems of mathematical physics the necessary complete set of physically adequate boundary conditions is absent. For example, in meteorological models (see e.g. [12–14]) we need boundary conditions at the upper computational level $p = \text{const} > 0$, but no boundary condition can describe the variety of very complex meteorological phenomena that occur in the upper atmosphere (above the layer essential to the task of forecasting for one week). On the other hand, we cannot use the pressure level $p = 0$ in the models, since we do not have steady measurements in the upper atmosphere, and the gas dynamics approximation becomes inadequate here. However, the upper boundary condition is necessary for the closure of both the differential and the finite-difference problems. Here the transparent boundary condition is a reasonable compromise. The corresponding ADTBC (see [19]) decreases the forecasting error in comparison with “simple” boundary conditions.

Also, in the problem of weather forecasting for a limited area V , we can use a “simple” approach and set Dirichlet boundary conditions at the border ∂V , where the right-hand side of the conditions is taken from a larger scale (global) forecasting

model. We can consider the difference between meteorological fields in these two numerical models. The dynamics of this difference (which is a vector-function) show that waves coming out of the computational area are reflected from the boundary ∂V . It is not a physical effect, which worsens the regional model's forecasts.

To obtain a mathematically correct mixed initial-boundary problem for the differential system, the number M of boundary conditions (according to the Shapiro – Lopatinsky theory, see [2–7]) may be smaller than the number of unknown functions. Moreover, for the perfect gas (with constant heat capacity and without dissipation) dynamics, the number M depends on the orientation of the wind direction at any boundary point $\vec{x} \in \partial V$. The number of boundary conditions for the corresponding dissipative (viscous) models is equal to the number of the unknown functions in the model.

Note 1. On the contrary, the Dirichlet boundary conditions for usual finite-difference approximations of the gas dynamic system provide the existence and uniqueness of the mixed problem's solution. However, the dissimilarity of these similar differential and finite-difference problems, significantly obstruct the convergence of finite-difference solutions when the steps of a finite-difference scheme tend to zero.

If we approximate a differential equation or a system using finite-difference schemes, the deficit of physically based boundary conditions may increase. For instance, if we use the finite-difference spatial approximation of the ideal gas dynamic's differential equations, according to the central difference formula, the number of boundary conditions required for the uniqueness of the solution increases in comparison with the differential problem. For the transport equation with viscosity, phenomena such as a boundary layer on the outflow from the region may occur.

Such computational difficulties are usually overcome by introducing into the algorithm a special finite-difference operator of a large computational viscosity in some vicinity of the boundary. However, it inevitably leads to an increase of the prediction error.

Note 2. To avoid the non-physical reflection in such boundary problems it is necessary to construct an analogue of the famous Sommerfeld radiation condition for the Helmholtz equation $\Delta u + k^2 u = 0$, see e.g. [23,24]. The asymptotical condition (as $r \equiv |\vec{x}| \rightarrow \infty$)

$$\partial_r u - iku = o(r^{-1})$$

guarantees the solution's uniqueness of the Helmholtz equation in the whole space \mathbb{R}^m .

Some types of linear evolutionary partial differential equations may be reduced to stationary differential equations (e.g., the wave equation to the Helmholtz one – for the Cauchy's problem using the Laplace transform, or, if the solution is assumed to be harmonic with respect to time, using the Fourier transform). This asymptotical Sommerfeld condition may be developed for some other PDEs (and systems).

The accuracy order of the asymptotical condition may be improved, if suitable terms with higher order derivatives are added. The conditions may be approximated by finite-difference formulae.

Note 3. The term Artificial (or Absorbing) Boundary Conditions (ABC) is also known as boundary conditions Imitating Cauchy Problem (ICP), full absorption conditions, computational boundary conditions, transparent boundary conditions, radiation boundary conditions, open boundary conditions, etc., see e.g. [25,26]. The properties of such boundary conditions were discussed and compared in [27–31].

Let us consider a linear differential equation with partial derivatives that is correct by Petrovsky (see [16,32]):

$$\partial_t \vec{u} = A \vec{u} + \vec{f}, \quad (6)$$

where $A = A(\partial_{\vec{x}})$ is a linear differential operator in \mathbb{R}^m , \vec{f} is a given function (forcing). We consider Eq. (6) in area $V \subset \mathbb{R}^m$ with piece-smooth boundary ∂V . To determine a unique solution of Eq. (6) Cauchy initial conditions are posed:

$$\vec{u}(t, \vec{x})|_{t=0} = \vec{u}_0(\vec{x}).$$

The given functions $\vec{f}(\vec{x})$, $\vec{u}_0(\vec{x})$ with supports in V , may be extended into the whole space by zeros and the Cauchy problem for Eq. (6) may be considered for \mathbb{R}^m . Let us use this solution as a reference. We say that a set of boundary conditions imitate the Cauchy problem, if for all \vec{u}_0 and \vec{f} the solution of Eq. (6) in the area V under these boundary conditions is equivalent to the reference solution with extended by zero functions $\vec{f}(\vec{x})$ and $\vec{u}_0(\vec{x})$.

Note 4. The definition may be extended for the cases of differential equations with a higher differential order with respect to time t and, moreover, non-resolved with respect to the highest time derivative. Eq. (1) is an example of such a differential equation. However, first we briefly describe TBCs for several classical linear PDEs to facilitate understanding (see e.g. [9,11,16–18,20,22,33–37]).

The reference solution may be obtained for such functions \vec{f} , \vec{u}_0 , if the Green functions (fundamental solutions, kernels, etc.) of Eq. (6) are known. Since $\text{supp } \vec{f} \subseteq \bar{V}$ and $\text{supp } \vec{u}_0 \subseteq \bar{V}$, we restrict the relative integrals over \mathbb{R}^m in these formulae on the area V and obtain for $\vec{x} \in V$:

$$\vec{u}(t, \vec{x}) = \int_V K_1(t, \vec{x} - \vec{y}) \vec{u}_0(\vec{y}) d\vec{y} + \int_0^t \int_V K_2(t - s, \vec{x} - \vec{y}) \vec{f}(s, \vec{y}) d\vec{y} ds. \quad (7)$$

For instance, for the scalar diffusion equation $\partial_t u = D \Delta u + f$ the scalar Green functions are:

$$K_1(t, \vec{x} - \vec{y}) = \frac{1}{(\sqrt{4\pi Dt})^m} \exp\left(-\frac{|\vec{x} - \vec{y}|^2}{4Dt}\right), \quad K_2(t - s, \vec{x} - \vec{y}) = \frac{1}{(\sqrt{4\pi D(t-s)})^m} \exp\left(-\frac{|\vec{x} - \vec{y}|^2}{4D(t-s)}\right). \quad (8)$$

The famous Poisson integral formula, as well as integral formulae (convolutions) for other classical equations of mathematical physics with constant coefficients, may be obtained by the Fourier transform. They give an exact solution of the Cauchy problem for arbitrary initial data and right hand sides such that $\text{supp } \vec{f} \subseteq V$, $\text{supp } \vec{u}_0 \subseteq V$. The transparent boundary conditions should provide the same solution for mixed problem in $x \in V, t \geq 0$.

The kernels K_1 and K_2 decrease exponentially with respect to spatial variables. However, the practical computation of integrals (7) may be computationally expensive.

Although the Green functions exist for equations with variable coefficients, their explicit practical determination is very difficult. The finite-difference approach for the special mixed initial-boundary problem is more preferable, although its implementation is associated with noticeable difficulties.

Sommerfeld's condition is fulfilled only asymptotically as $|\vec{x}| \rightarrow \infty$. On the contrary, we define and construct boundary conditions on ∂V , i.e. in concrete points, lines, or planes. We consider the cases, where ∂V is one or two points, one or two parallel lines, or planes.

Let the variable x_1 be normal to the boundary, $\vec{x} = \langle x_1, \vec{y} \rangle$, $\dim \vec{x} = \dim \vec{y} + 1$. To obtain TBC, we have to give up the locality property (inherent, e.g., in the Sommerfeld condition for the wave equation) and include non-local integral operators of the convolution type. Let $V = \mathbb{R}_+^m$, $x_1 > 0$. The integrals provide participation in such boundary conditions at an arbitrary time moment $t > 0$ and in an arbitrary border point $\vec{y} \in \partial V$ of the solution's boundary values at all previous time moments $0 \leq s \leq t$ and at $\vec{z} \in \partial V$, i.e. the boundary condition takes the form:

$$\partial_{x_1} u(t, 0, \vec{y}) = \int_0^t \int_{\mathbb{R}^{m-1}} K(t-s, \vec{y}-\vec{z}) u(s, 0, \vec{z}) d\vec{z} ds, \quad (9)$$

or

$$\partial_{x_1} u(t, 0, \vec{y}) = Q(\partial_{\vec{y}}) u(t, 0, \vec{y}) + \int_0^t \int_{\mathbb{R}^{m-1}} K(t-s, \vec{y}-\vec{z}) u(s, 0, \vec{z}) d\vec{z} ds, \quad (10)$$

or more general integro-differential operator

$$\partial_{x_1} u(t, 0, \vec{y}) = Q(\partial_{\vec{y}}) u(t, 0, \vec{y}) + \sum_{\kappa} \int_0^t \int_{\mathbb{R}^{m-1}} K_{\kappa}(t-s, \vec{y}-\vec{z}) Q_{\kappa} u(s, 0, \vec{z}) d\vec{z} ds, \quad (11)$$

where Q and Q_{κ} are differential operators with respect to time and spatial variables that are tangential to the boundary. Here, we may have several terms with different differential operators and kernels – the indexes of such terms are denoted by κ . The forms of these differential operators and kernels K_{κ} are determined by the original operator A (see examples, e.g., in [16,38]).

Boundary conditions Eqs. (9)–(11) can imitate the Cauchy's problem with initial values and right hand side being prolonged with zeros. If the values of given functions $u_0(\vec{x})$ and $f(t, \vec{x})$ outside of the computational domain are nonzero, then the boundary condition Eq. (9)–(11) should be supplemented with terms that describe their contribution.

The TBCs for the one dimensional wave equation

$$\partial_t^2 u = c^2 \partial_x^2 u$$

on the segment $[-1, 1]$ are local:

$$\partial_t u = \pm c \partial_x u.$$

Usually TBCs are non-local. For instance, for the diffusion equation in the half-space $x \geq 0$, $\vec{y} \in \mathbb{R}^{m-1}$ we obtain the following TBC:

$$u(t, 0, \vec{y}) = 2^{1-m} \pi^{-m/2} D^{1-m/2} \int_0^t \int_{\mathbb{R}^{m-1}} \exp \left[\frac{|\vec{y}-\vec{y}'|^2}{4D(t-s)} \right] \partial_x u(s, 0, \vec{y}') \frac{d\vec{y}' ds}{(t-s)^{m/2}}.$$

For the multidimensional problems the TBC for wave equations in the area $x > 0$ at dimensions $m = 2, 3$ we have

$$\partial_x u(t, 0, y) = \frac{2c}{\sqrt{\pi}} \int_0^t \int_{|y-y'| \leq c(t-s)} \frac{[c^{-2} \partial_s^2 - \partial_{y'}^2] u(s, 0, y')}{\sqrt{c^2(t-s)^2 - |y-y'|^2}} dy' ds.$$

and

$$\partial_x u(t, 0, y, z) = \frac{2c}{\sqrt{\pi}} \int_0^t \int_{|y-y'|^2 + |z-z'|^2 \leq c^2(t-s)^2} [c^{-2} \partial_s^2 - \partial_{y'}^2] u(s, 0, y', z') dy' dz' ds.$$

Note 5. Sometimes the integration area in Eq. (9) may be reduced. For instance, in the case of hyperbolic equations in the half-space \mathbb{R}_+^m the kernel's support is included into the inverse light cone $|\vec{y}-\vec{z}| \leq c(t-s)$, where the constant c is the speed of light, m is odd, the kernel's support in these formulae may be reduced (by the Stokes formula) to the boundary of the inverse light cone $|\vec{y}-\vec{z}| = c(t-s)$, i.e. we obtain a lacuna (see for comparison [39]). The explicit formulae for TBC for other evolutionary partial derivative equations and systems of mathematical physics were considered in [12], see also [16].

Note 6. Sometimes there is a finite-difference analogue of the inverse light cone for hyperbolic differential equations and Sys. (6). The DTBCs and ADTBCs were constructed in [12] for explicit and “almost explicit” finite-difference schemes for

the 2D wave equation, and the linearised shallow water system (barotropic model) with the Coriolis parameter. The DTBCs were constructed in the form of discrete convolutions with respect to time t and 1D tangential (to the boundary) variable y . It is a scalar operator for the wave equation, and a matrix (3×3) operator for shallow water systems. The kernels of the convolutions were determined numerically. The inverse light cone was observed in both examples: the supports of the kernels are included in the cones, if the explicit schemes are stable (the Courant – Friedrichs – Lewy criterion is fulfilled).

Artificial boundary conditions for a finite area V were studied using Calderon's integral operators in [33–36]. DTBCs for Leontovich equation (which may be reduced to the Schrödinger equation) were constructed in [37] for cuboid V by using the Fresnel transform.

3. Finite-difference implicit scheme

Let us consider Eq. (1) with constant coefficients ρ, R, E and with zeroth forcing f :

$$\rho \frac{\partial^2 u}{\partial t^2} - R^2 \rho \frac{\partial^4 u}{\partial t^2 \partial x^2} + ER^2 \frac{\partial^4 u}{\partial x^4} = 0, \quad (12)$$

and the implicit finite-difference scheme on the five-point stencil of the Crank – Nicolson type that approximates Eq. (12) on a uniform grid with the steps τ with respect to time t and h with respect to spatial variable x :

$$\sigma (u_{m+2}^{n+1} + u_{m-2}^{n+1} + u_{m+2}^{n-1} + u_{m-2}^{n-1}) + \beta (u_{m+1}^{n+1} + u_{m-1}^{n+1} + u_{m+1}^{n-1} + u_{m-1}^{n-1}) + \alpha (u_m^{n+1} + u_m^{n-1}) + \gamma (u_{m-1}^n + u_{m+1}^n) + \delta u_m^n = 0, \quad (13)$$

where the upper index n corresponds to the number of the time step, and the lower index m corresponds to the spatial variable, $m = 2, 3, \dots, N-2$, where $N+1$ is the number of grid points in the segment $[-L/2, L/2]$. Thus, we define $N-3$ linear algebraic equations with $N+1$ unknown values $\{u_m^{n+1}\}_{m=0}^N$. The coefficients of the scheme are deduced using dimensionless parameters $\nu = ER^2 \rho^{-1} \cdot \tau^2 h^{-4}$, $\mu = R^2 \cdot h^{-2}$ and formulae $\alpha = 1 + 3\nu + 2\mu$, $\beta = -2\nu - \mu$, $\gamma = 2\mu$, $\delta = -2 - 4\mu$, $\sigma = \nu/2$.

To close the linear algebraic system we must add two linear algebraic equations that describe two boundary conditions on the left edge of the segment and, similarly, the same number of equations for the right edge. As a result, we obtain a closed linear algebraic system for $\{u_m^{n+1}\}_{m=0}^N$.

To begin the computational process and calculate the values $\{u_m^2\}_{m=0}^N$, we need two initial functions $\{u_m^0\}_{m=0}^N$ and $\{u_m^1\}_{m=0}^N$.

4. Discrete transparent boundary conditions, rational approximations, stability

4.1. Derivation of DTBCs for finite-difference equations

Consider an ordinary finite-difference equation of degree n with constant coefficients

$$a_n u(m+n) + \dots + a_0 u(m) = g(m), \quad m \in \mathbb{Z}, \quad (14)$$

where $g(m)$ is a given right hand side, which decreases as $m \rightarrow \pm \infty$. Further, consider the fundamental set of solutions as $g(m) \equiv 0$. If all roots of the characteristic equation

$$a_n \lambda^n + \dots + a_0 = 0 \quad (15)$$

are different, then the fundamental set of solutions of Eq. (14) can be expressed as $Y_k(m) = \text{const}_k \cdot \lambda_k^m$, $k = 1, \dots, n$, where λ_k are the solutions of Eq. (15). If some roots are multiple, we also have solutions $m^d \lambda_k^m$, where the degree d is less than the multiplicity of the corresponding root λ_k . We also assume that the boundary is not characteristic, i.e. there are no roots of Eq. (15) such that $|\lambda_k| = 1$.

Solutions of Eq. (14) that are bounded as $m \rightarrow \infty$ could be expressed as (see, e.g. [40])

$$u(m) = \sum_{j=-\infty}^{\infty} G(m, j) g(j), \quad (16)$$

where the kernel G (Green function) is constructed using the fundamental set of solutions on the real line.

Green's function (built by the fundamental set of solutions) is used to justify the algorithm of construction of DTBCs, see [12,14,22]. For Schrödinger, wave, diffusion equations, and Eq. (1) this fundamental set of solutions can be divided into two parts – half of the solutions decreases as $x \rightarrow \infty$, the other half decreases as $x \rightarrow -\infty$. The similar statement is true for finite-difference equations, i.e. as $m \rightarrow \pm \infty$.

Let K be the number of roots of characteristic equation Eq. (15) satisfying the inequality $|\lambda| < 1$, i.e.

$$|\lambda_1| \leq \dots \leq |\lambda_K| < 1 < |\lambda_{K+1}| \leq \dots \leq |\lambda_n|.$$

If we consider a partial differential equation, then the Fourier (and / or Laplace) transform should be applied to all variables that are tangential to the boundary (including time t), see [11]. For finite-difference equations, the analogous discrete transforms are used. The functions Y_k are also dependent on dual variables. We assume that the number K does not depend on the dual variables, i.e. the border is not characteristic. In Eq. (13), we only have one variable (time) that is tangential to the boundary.

If we consider the problem on the positive discrete half-line $m \geq 0$, then the summation in Eq. (16) is done only for non-negative indexes j . The kernel $G(m, j)$ remains the same (i.e. the solution of mixed problem for all decreasing functions $g(m)$ as $m \rightarrow \infty$), if at $m = 0$ there are such K boundary conditions that the functions of fundamental set of solutions are not changed. In other words, with such boundary conditions, the solution of the problem on the positive discrete half-line will coincide with the solution on the real line for $j \geq 0$. Therefore, such K boundary conditions imitate the bounded solution at $-\infty$, meaning that there is no reflection from the left boundary at $m = 0$.

To obtain this transparency property on the left border of Eq. (14), it is sufficient (see proof by author in [11] or [12–14]) to construct homogeneous boundary conditions at point $m = 0$, such that

1. functions $Y_k(m)$ satisfy the conditions for all $k > K$;
2. linear combination $\sum_{k=1}^K \text{const}_k Y_k(m)$ satisfies the boundary conditions if and only if $\text{const}_k = 0$, $\forall k = 1, \dots, K$.

Note 7. To obtain the transparency property on the right border, the inequality sign in the requirement 1. should be changed to $k \leq K$, and the index k in the requirement 2. (as well as the summation) is now from $K + 1$ to n .

The requirement 1. may be interpreted as an orthogonality condition in the space of linear boundary operators. The codimension of the subspace is equal to $n - K$.

Note 8. The requirement 2. is the discrete analogue of famous Shapiro – Lopatinsky condition for differential equations. It can be formulated in the following form. Let us consider the matrix $\|I_{ij}\|_{i,j=1}^K$, where I_{ij} is the value of i -th boundary operator on Y_j . Its determinant (Lopatinsky determinant of the boundary problem) must be nonzero. The similar Lopatinsky determinant may be constructed for various differential problems (instead of the finite-difference).

Later in Section 4.4 we apply rational approximations of DTBCs to obtain ADTBC. Therefore, the corresponding Lopatinsky determinant will almost always be nonzero. To check the stability of mixed problem with applied ADTBCs, we propose other approach described in Section 4.5.

The requirements 1. and 2. do not define unique boundary conditions. The suitable gauge could be chosen in the space of boundary conditions – in practice, specific boundary operators. We explain our choice of the gauge in Section 4.4.

If the problem is considered on a segment, then the boundary conditions that imitate the Cauchy problem are used on each edge. The total number of boundary conditions at both edges is equal to n . In this work, we have $n = 4$ and $K = 2$ (see Section 4.3).

4.2. General plan of approach

The algorithm for constructing ADTBCs at $x = \pm L/2$ for Eq. (13) is as follows:

- Step 1. Apply the \mathcal{Z} -transformation (discrete analogue of the Laplace integral transformation) with respect to time to Eq. (13) and obtain a linear ordinary finite-difference equation with respect to the spatial variable m ; the coefficients of the equation depend on the parameter $z \in \mathbb{C}$.
- Step 2. Construct, for the corresponding homogeneous finite-difference 4th order equation, a fundamental set of solutions $\{Y_j(m)\}_{j=1}^4$, such that solutions Y_1, Y_2 decrease as $m \rightarrow +\infty$, and solutions Y_3, Y_4 decrease as $m \rightarrow -\infty$.
- Step 3. Decompose the obtained growing (as $m \rightarrow +\infty$) solutions (functions from the dual variable z with respect to time t) into a series in a neighbourhood of $z = \infty$.
- Step 4. Construct vectorial rational functions (the construction generalises the Hermite – Padé approximation at the point $z = \infty$, see e.g. [14,16,21,22,41]), which are asymptotically orthogonal to two growing solutions of this \mathcal{Z} -transformed equation. The corresponding polynomials are symbols of the transparent boundary operators.
- Step 5. Apply the inverse \mathcal{Z} -transformation to the obtained coefficients of the convolution operators in ADTBCs.

In order to calculate the inverse \mathcal{Z} -transformation, it is necessary to decompose the symbols of the corresponding operators into a Laurent series in the neighbourhood of the point $z = \infty$. For convenience, we introduce a change of variable: $\omega = 1/z$ and decompose the symbols into a Taylor series in the neighbourhood of the point $\omega = 0$.

The growth and decrease of the Taylor coefficients of the meromorphic function are associated with the location of the function singularities on the complex plane. It is important to estimate the areas of the convergence of the obtained power series, which depend on the features of functions (solutions of the homogeneous finite-difference equation). The singularities are either points of pole, or branch points.

4.3. Transparent boundary conditions for the finite-Difference equation

Let us apply the \mathcal{Z} -transformation with respect to time to Eq. (13). Then we obtain the linear ordinary non-homogeneous finite-difference equation

$$\sigma(z^2 + 1)[v(m+4) + v(m)] + (\beta(z^2 + 1) + \gamma z)[v(m+3) + v(m+1)] + (\alpha(z^2 + 1) + \delta z)v(m+2) = g(z, m), \quad (17)$$

where $z \in \mathbb{C}$ is the variable that is dual to the discrete time n , $v(m) \equiv v(m, z)$ is the image of the solution u_m^n , and $g(z, m)$ is the right hand side that is obtained by the \mathcal{Z} -transformation from the initial functions u_m^0 and u_m^1 . If we approximate non-homogeneous Eq. (1), then the image of the \mathcal{Z} -transformation of the right hand side f is included in $g(z, m)$.

The corresponding homogeneous equation after the change of variable $\omega = 1/z$ has the form

$$\sigma(\omega^2 + 1)[v(m+4) + v(m)] + (\beta(\omega^2 + 1) + \gamma\omega)[v(m+3) + v(m+1)] + (\alpha(\omega^2 + 1) + \delta\omega)v(m+2) = 0. \quad (18)$$

The order of the characteristic equation for ordinary finite-difference Eq. (18) (see e.g. [14,16,18,20,22,40])

$$\sigma(1 + \omega^2)[\lambda^4 + 1] + (\beta(1 + \omega^2) + \gamma\omega)[\lambda^3 + \lambda] + (\alpha(1 + \omega^2) + \delta\omega)\lambda^2 = 0 \quad (19)$$

at $\omega \neq \pm i$ is equal to 4 and is reciprocal. Let us divide Eq. (19) by λ^2 and rewrite it in the form

$$\sigma(1 + \omega^2)[\lambda + \lambda^{-1}]^2 + (\beta(1 + \omega^2) + \gamma\omega)[\lambda + \lambda^{-1}] + \delta\omega + (\alpha - 2\sigma)(1 + \omega^2) = 0. \quad (20)$$

Note 9. The order of algebraic Eq. (19) at $\omega = \pm i$ is equal to 3:

$$\gamma\omega(\lambda^3 + \lambda) + \delta\omega\lambda^2 = 0.$$

Therefore, $\lambda_1 = 0$, and as $\omega \rightarrow \pm i$ we obtain $\lambda_3 \rightarrow \infty$. Here the numbering of functions λ_i is the same as in non-degenerate case Eq. (19). We determine the remaining two roots of the cubic equation from the quadratic reciprocal equation:

$$\lambda^2 + \frac{\delta}{\gamma}\lambda + 1 = 0,$$

where $\delta/\gamma = -2 - 1/\mu$, and therefore

$$\lambda_{2,4} = 1 + \frac{1}{2\mu} \mp \sqrt{\left(1 + \frac{1}{2\mu}\right)^2 - 1}.$$

Thus, both roots are real and positive. According to Vieta's theorem, the following inequalities are fulfilled:

$$0 < \lambda_2 < 1 < \lambda_4.$$

For other values of ω we change variable $\eta = \lambda + \lambda^{-1}$ in Eq. (20) and obtain a quadratic equation for the auxiliary variable η :

$$\sigma(1 + \omega^2)\eta^2 + (\beta(1 + \omega^2) + \gamma\omega)\eta + \delta\omega + (\alpha - 2\sigma)(1 + \omega^2) = 0. \quad (21)$$

The roots of Eq. (21) are

$$\begin{aligned} \eta_1(\omega) &= \frac{-\beta(1 + \omega^2) - \gamma\omega - \sqrt{(\beta(1 + \omega^2) + \gamma\omega)^2 - 4\sigma(1 + \omega^2)[\delta\omega + (\alpha - 2\sigma)(1 + \omega^2)]}}{2\sigma(1 + \omega^2)}, \\ \eta_2(\omega) &= \frac{-\beta(1 + \omega^2) - \gamma\omega + \sqrt{(\beta(1 + \omega^2) + \gamma\omega)^2 - 4\sigma(1 + \omega^2)[\delta\omega + (\alpha - 2\sigma)(1 + \omega^2)]}}{2\sigma(1 + \omega^2)}, \end{aligned} \quad (22)$$

where $\sqrt{\cdot}$ is the complex root with a positive real part of $y \in \mathbb{C} \setminus \mathbb{R}_-$.

Before decomposing the functions $\lambda_j(\omega)$, $j = 1, 4$ into Taylor series in a vicinity of the origin $\omega = 0$, we do it for the auxiliary functions $\eta_1(\omega), \eta_2(\omega)$, see Appendix A:

$$\eta_1(\omega) = \frac{1}{v} \sum_{k=0}^{\infty} (-1)^k \omega^{2k} \left[(\mu + 2v)(1 + \omega^2) - 2\mu\omega - \sqrt{\mu^2 - 2v}(1 - \omega) \left(\omega^2 - 2 \frac{\mu^2}{\mu^2 - 2v} \omega + 1 \right) \sum_{n=0}^{\infty} P_n \left(\frac{\mu^2}{\mu^2 - 2v} \right) \omega^n \right], \quad (23)$$

$$\eta_2(\omega) = \frac{1}{v} \sum_{k=0}^{\infty} (-1)^k \omega^{2k} \left[(\mu + 2v)(1 + \omega^2) - 2\mu\omega + \sqrt{\mu^2 - 2v}(1 - \omega) \left(\omega^2 - 2 \frac{\mu^2}{\mu^2 - 2v} \omega + 1 \right) \sum_{n=0}^{\infty} P_n \left(\frac{\mu^2}{\mu^2 - 2v} \right) \omega^n \right], \quad (24)$$

where $P_n(\varepsilon)$ is a Legendre polynomial of degree n at point ε . The computation algorithm of Legendre polynomials is described in Appendix C.

Asymptotic of the functions as $\omega \rightarrow 0$ are described by the formulae

$$\begin{aligned} \eta_1(\omega) &= \vartheta_1 + r_1(\omega), \\ \eta_2(\omega) &= \vartheta_2 + r_2(\omega), \end{aligned} \quad (25)$$

where $r_j(\omega) \rightarrow 0$, $j = 1, 2$, and

$$\begin{aligned}\vartheta_1 &= \frac{1}{2\sigma} \left[\beta - \sqrt{\beta^2 - 4\sigma(\alpha - 2\sigma)} \right] = 2 + \frac{\mu}{\nu} - \frac{1}{\nu} \sqrt{\mu^2 - 2\nu}, \\ \vartheta_2 &= \frac{1}{2\sigma} \left[\beta + \sqrt{\beta^2 - 4\sigma(\alpha - 2\sigma)} \right] = 2 + \frac{\mu}{\nu} + \frac{1}{\nu} \sqrt{\mu^2 - 2\nu}.\end{aligned}\quad (26)$$

If the inequality $\mu^2 > 2\nu$ is fulfilled, i.e. if

$$\tau < R\sqrt{\frac{\rho}{2E}}, \quad (27)$$

then the radicand in Eq. (26) is positive, and the values ϑ_1, ϑ_2 are real.

Let us resolve the relation $\eta = \lambda + \lambda^{-1}$ as a quadratic equation

$$\lambda^2 - \eta\lambda + 1 = 0. \quad (28)$$

For both η_1, η_2 we obtain the following roots of characteristic Eq. (19):

$$\begin{aligned}\lambda_1 &= \frac{\eta_1(\omega)}{2} - \sqrt{\frac{\eta_1^2(\omega)}{4} - 1}, & \lambda_2 &= \frac{\eta_2(\omega)}{2} - \sqrt{\frac{\eta_2^2(\omega)}{4} - 1}, \\ \lambda_3 &= \frac{\eta_1(\omega)}{2} + \sqrt{\frac{\eta_1^2(\omega)}{4} - 1}, & \lambda_4 &= \frac{\eta_2(\omega)}{2} + \sqrt{\frac{\eta_2^2(\omega)}{4} - 1}.\end{aligned}$$

Note 10. According to Vieta's theorem, either the absolute values of both roots of Eq. (28) are equal to 1, or one absolute value is smaller than 1 and the other one is greater. The first version takes place, if $\eta \in [-2, 2] \subset \mathbb{R}$. As $\omega \rightarrow 0 \in \mathbb{C}$ this can never be obtained. Indeed, if inequality (27) is fulfilled, the square roots in Eq. (26) are real and $2 < \vartheta_1 < \vartheta_2$. If the equality $\mu^2 = 2\nu$ is fulfilled, then $2 < \vartheta_1 = \vartheta_2$. If the inequality, which is inverse to (27) is fulfilled, then the values ϑ_1, ϑ_2 are not real. Thus, at small ω we obtain $\eta_{1,2} \notin [-2, 2]$, i.e. the necessary condition of the mixed initial-boundary problem correctness for the finite-difference Eq. (13) is fulfilled.

The Taylor series of functions $\lambda_i(\omega)$ at point $\omega = 0$ have the forms (see Appendix B)

$$\lambda_{1,3}(\omega) = \frac{\eta_1(\omega)}{2} \mp \sqrt{\frac{\vartheta_1^2}{4} - 1} \cdot \sum_{n=0}^{\infty} \frac{(-1)^n (2n)! r_1^n(\omega)}{(1-2n)n! 4^n (\theta_1+2)^n} \cdot \sum_{n=0}^{\infty} \frac{(-1)^n (2n)! r_1^n(\omega)}{(1-2n)n! 4^n (\theta_1-2)^n}, \quad (29)$$

$$\lambda_{2,4}(\omega) = \frac{\eta_2(\omega)}{2} \mp \sqrt{\frac{\vartheta_2^2}{4} - 1} \cdot \sum_{n=0}^{\infty} \frac{(-1)^n (2n)! r_2^n(\omega)}{(1-2n)n! 4^n (\theta_2+2)^n} \cdot \sum_{n=0}^{\infty} \frac{(-1)^n (2n)! r_2^n(\omega)}{(1-2n)n! 4^n (\theta_2-2)^n}, \quad (30)$$

where $\eta_1(\omega)$, $\eta_2(\omega)$ and $r_{1,2}(\omega)$ are taken from Eqs. (23), (24) and (25), respectively.

The following inequalities are fulfilled as $\omega \rightarrow 0$

$$|\lambda_1|, |\lambda_2| < 1 < |\lambda_3|, |\lambda_4|.$$

Therefore, as $m \rightarrow +\infty$ it is possible to derive decreasing λ_1^m , λ_2^m and increasing λ_3^m , λ_4^m solutions of finite-difference Eq. (18), which form the fundamental set of solutions.

4.4. Transparent boundary conditions and rational approximations

As with differential Eq. (12), for the correctness of the mixed initial-boundary value problem for finite-difference Eq. (13), two boundary conditions at each edge of the rod are required. Thus, the values of the solution u at boundary and several preboundary grid points should be calculated at every time step. We start by constructing the \mathcal{Z} -image of the boundary conditions for the left edge in the form:

$$\begin{aligned}P_1(\omega) v(0) + Q_1(\omega) v(1) + R_1(\omega) v(2) + S_1(\omega) v(3) &= 0, \\ P_2(\omega) v(0) + Q_2(\omega) v(1) + R_2(\omega) v(2) + S_2(\omega) v(3) &= 0,\end{aligned}$$

which (after the inverse \mathcal{Z} -transformation) corresponds to the relations

$$\sum_{j=0}^{\infty} p_{kj} u_0^{n-j} + \sum_{j=0}^{\infty} q_{kj} u_1^{n-j} + \sum_{j=0}^{\infty} r_{kj} u_2^{n-j} + \sum_{j=0}^{\infty} s_{kj} u_3^{n-j} = 0, \quad k = 1, 2, \quad (31)$$

where values p_{kj} , q_{kj} , r_{kj} and s_{kj} are the coefficients in Taylor series before the term ω^j of the functions $P_k(\omega)$, $Q_k(\omega)$, $R_k(\omega)$, $S_k(\omega)$, respectively ($k = 1, 2$) in a vicinity of the point $\omega = 0 \in \mathbb{C}$. The requirements 1. and 2. from Section 4.1 must be fulfilled for all ω in the vicinity of zero.

Two (with numbers $k = 1, 2$) linearly independent boundary conditions will provide the transparency property, if and only if for the increasing Cauchy problem solutions $v(m) = \lambda_3^m$ and $v(m) = \lambda_4^m$ the symbols of the boundary conditions $\langle P_1, Q_1, R_1, S_1 \rangle$ and $\langle P_2, Q_2, R_2, S_2 \rangle$ fulfill the following equations:

$$P_k + Q_k \lambda_3 + R_k \lambda_3^2 + S_k \lambda_3^3 = 0,$$

$$P_k + Q_k \lambda_4 + R_k \lambda_4^2 + S_k \lambda_4^3 = 0. \quad (32)$$

Note 11. Here we compose spatial stencils for the boundary conditions from 4 points with respect to m : $-L/2$, $-L/2 + h$, $-L/2 + 2h$, $-L/2 + 3h$. However, more space steps could be included:

$$\sum_{i=0}^I P_{k,i} \lambda_3^i = 0,$$

$$\sum_{i=0}^I P_{k,i} \lambda_4^i = 0.$$

Here, I is a number of space steps used in the boundary conditions, $P_{k,i} \equiv P_{k,i}(\omega)$ are polynomials, index k corresponds to number of boundary condition ($k = 1$ for the first boundary condition and $k = 2$ for the second one), and index i corresponds to the space step ($i = 0$ for boundary layer, $i = 1$ for preboundary layer, etc).

For any given values ω the subspace of solutions of System (32) is two-dimensional and two boundary conditions on every edge can provide a boundary problem correctness for finite-difference Eq. (17). However, the subspace of the solutions of System (32) in the space of analytic vector-functions of ω is infinity-dimensional.

The meromorphic functions $\lambda_3(\omega)$, $\lambda_4(\omega)$ are not rational, and usually solutions of System (32) in the subspace of polynomials do not exist. Therefore, DTBCs are non-local with respect to time. They include values of the solution of the boundary problem for Eq. (13) in the infinite number of previous time moments. For such a realisation of the ADTBCs the number of arithmetic operations, as well as the necessary computer memory, is proportional to the number of the temporal steps n . We say that the boundary conditions are local with respect to time, if there exists a fixed natural number n_t (number of time steps), such that at any time step $T = n\tau$, $n \in \mathbb{N}$ the boundary value is calculated only by using several preboundary points at the times $n\tau$, $(n-1)\tau$, $(n-2)\tau$, ..., $(n-n_t+1)\tau$.

That is why we relax the requirements for the symbols of the operators of DTBCs, and exchange unknown analytic functions in System (32) by polynomials and exact equalities by asymptotic (as $\omega \rightarrow 0$ and $k = 1, 2$):

$$\begin{cases} P_k(\omega) + Q_k(\omega) \lambda_3(\omega) + R_k(\omega) \lambda_3^2(\omega) + S_k(\omega) \lambda_3^3(\omega) = O(\omega^{K_k}), \\ P_k(\omega) + Q_k(\omega) \lambda_4(\omega) + R_k(\omega) \lambda_4^2(\omega) + S_k(\omega) \lambda_4^3(\omega) = O(\omega^{K_k}). \end{cases} \quad (33)$$

The “physical” interpretation of the exchange: we neglect the impact of solution’s values for the distant past, assuming the resulting opacity is small. However the requirement 2. from Section 4.1 may be violated as the result of the exchange of System (32) to System (33). Then, the corresponding mixed problem will be incorrect.

We fix the degrees of the polynomials P_k , Q_k , R_k , and S_k , i.e. stencils for the ADTBCs. The number of the degrees of freedom in these four polynomials is equal to $M_k = \deg P_k + \deg Q_k + \deg R_k + \deg S_k + 4$, and the number of linear algebraic equations, which are obtained from System (33) is equal to $2K_k$. Together with two normalisation conditions, which will be considered below, we obtain $2K_k + 2$ linear algebraic equations. Thus, if $M_k = 2K_k + 2$ and the system of linear algebraic equations is non-degenerate, we determine a unique set of the polynomials P_k , Q_k , R_k , and S_k with given degrees.

If we choose normalisation condition at $k = 1$:

$$P_1(0) = p_{1,0} = 1, \quad Q_1(0) = q_{1,0} = 0,$$

then we are able to compute the value u_0^n for every temporal step n using the values in the inner points u_{2h}^j , u_{3h}^j at $j \leq n$ and in the border and preborder points at previous time moments: u_0^j , u_1^j at $j < n$. Thus, we obtained the first boundary condition in the form:

$$u_0^n + \sum_{j=1}^{\deg P_1} p_{1j} u_0^{n-j} + \sum_{j=1}^{\deg Q_1} q_{1j} u_1^{n-j} + \sum_{j=0}^{\deg R_1} r_{1j} u_2^{n-j} + \sum_{j=0}^{\deg S_1} s_{1j} u_3^{n-j} = 0. \quad (34)$$

If we choose normalisation condition at $k = 2$:

$$P_2(0) = p_{2,0} = 0, \quad Q_2(0) = q_{2,0} = 1,$$

then we are able to compute the value u_1^n for every temporal step n using the values in the inner points u_2^j , u_3^j at $j \leq n$ and in the border and preborder points at previous time moments: u_0^j , u_1^j at $j < n$. So, we obtain the second ADTBCs:

$$u_1^n + \sum_{j=1}^{\deg P_2} p_{2j} u_0^{n-j} + \sum_{j=1}^{\deg Q_2} q_{2j} u_1^{n-j} + \sum_{j=0}^{\deg R_2} r_{2j} u_2^{n-j} + \sum_{j=0}^{\deg S_2} s_{2j} u_3^{n-j} = 0. \quad (35)$$

Note 12. Conditions in System (33) are similar to the famous Hermite – Padé rational approximation of meromorphic functions. However, it is identical in the case of unique ADTBCs (see [14,16,21,22]). For two ADTBCs it is a more general vector rational approximation. Similar constructions, which can be considered as a generalisation of the Hermite – Padé rational approximation, were studied in [42].

The coefficients of System (33) are not real, because the functions $\lambda_3(\omega)$ and $\lambda_4(\omega)$ are, in general, complex. As a result, the characteristic values are complex conjugated, and we can transform the systems to the real form:

$$\begin{cases} P_1(\omega) + Q_1(\omega) \frac{\lambda_3(\omega) + \lambda_4(\omega)}{2} + R_1(\omega) \frac{\lambda_3^2(\omega) + \lambda_4^2(\omega)}{2} + S_1(\omega) \frac{\lambda_3^3(\omega) + \lambda_4^3(\omega)}{2} = O(\omega^{K_1}), \\ Q_1(\omega) \frac{\lambda_3(\omega) - \lambda_4(\omega)}{2i} + R_1(\omega) \frac{\lambda_3^2(\omega) - \lambda_4^2(\omega)}{2i} + S_1(\omega) \frac{\lambda_3^3(\omega) - \lambda_4^3(\omega)}{2i} = O(\omega^{K_1}), \\ P_1(0) = 1, Q_1(0) = 0, \end{cases} \quad (36)$$

at $k = 1$, and

$$\begin{cases} P_2(\omega) + Q_2(\omega) \frac{\lambda_3(\omega) + \lambda_4(\omega)}{2} + R_2(\omega) \frac{\lambda_3^2(\omega) + \lambda_4^2(\omega)}{2} + S_2(\omega) \frac{\lambda_3^3(\omega) + \lambda_4^3(\omega)}{2} = O(\omega^{K_2}), \\ Q_2(\omega) \frac{\lambda_3(\omega) - \lambda_4(\omega)}{2i} + R_2(\omega) \frac{\lambda_3^2(\omega) - \lambda_4^2(\omega)}{2i} + S_2(\omega) \frac{\lambda_3^3(\omega) - \lambda_4^3(\omega)}{2i} = O(\omega^{K_2}), \\ P_2(0) = 0, Q_2(0) = 1, \end{cases} \quad (37)$$

at $k = 2$.

We solve System (36) and System (37) separately and find the coefficients of the ADTBCs on the left edge of the rod. Using the same approach, we find coefficients for the ADTBCs on the right edge. The results of numerical experiments with such ADTBCs are presented in Section 5.

4.5. Stability of mixed problem with ADTBCs

The correctness (stability) of the Cauchy problem for a differential or finite difference equation does not guarantee that the mixed boundary value problem will also be correct. For stability, the boundary should be uncharacteristic and the boundary operators should satisfy the Shapiro – Lopatinsky conditions, see [2–7,13,14,16,22]. If the DTBCs were perfectly realised according to System (32), the solution of the mixed problem would coincide with the solution of the Cauchy problem, i.e. the problem would be stable. However, we are forced to implement the DTBCs according to System (36) and System (37), i.e. approximately. Thus, we need to check the stability of the mixed boundary value problem again. Here, we propose a numerical method to do so.

The Crank – Nicolson approximation Eq. (13) of the Cauchy problem for rod transverse vibrations Eq. (12) is absolutely stable (see Appendix D).

Usually, Chebyshev's norm in the space of grid functions is used to assess the stability of a finite-difference scheme:

$$\|u^n\|_C = \max_{0 \leq j \leq N} |u_j^n|, \quad (38)$$

where u_j^n is a grid function, n is the number of time step, j is the number of space step. Also, the approximation of L^2 norm is used (trapezoidal approximation):

$$\|u^n\|_{L^2} = \sqrt{h \left[\frac{1}{2} ((u_0^n)^2 + (u_N^n)^2) + \sum_{j=1}^{N-1} (u_j^n)^2 \right]}. \quad (39)$$

In the case of Eq. (1), the norms (38) and (39) of Cauchy problem's solution (in an infinite domain) may increase over time. At the same time, the energy norm (4) is preserved. Hence, the dynamic of a rod's energy is the key factor in the estimation of stability (finite-difference approximation and boundary conditions). For the finite domain $x \in [-L/2, L/2]$ for the model with ADTBCs at any time moment $t > 0$ this energy should be less than at time moment $t = 0$. This means that a part of the energy was transferred from the segment outside, i.e. there was no reflection from the boundaries.

In our experiments we use an approximation of Hamiltonian \mathcal{H} , see Eqs. (2) and (3), at the time moment $\tau(n + 1/2)$:

$$\hat{\mathcal{H}}[u^{n+1/2}] = h \left[\frac{1}{2} (\vartheta_0^{n+1/2} + \vartheta_N^{n+1/2}) + \sum_{j=1}^{N-1} \vartheta_j^{n+1/2} \right], \quad \|u^{n+1/2}\|_{\mathcal{H}} = \sqrt{\hat{\mathcal{H}}[u^{n+1/2}]}, \quad (40)$$

where for $j = 1, \dots, N-1$ we have

$$\vartheta_j^{n+1/2} = \rho \left(\frac{u_{j+1}^{n+1} - u_j^{n+1}}{\tau} \right)^2 + \rho R^2 \left(\frac{u_{j+1}^{n+1} - u_{j+1}^n - u_{j-1}^{n+1} + u_{j-1}^n}{2h\tau} \right)^2 + ER^2 \left(\frac{u_{j+1}^{n+1} - 2u_j^{n+1} + u_{j-1}^{n+1} + u_{j+1}^n - 2u_j^n + u_{j-1}^n}{2h^2} \right)^2,$$

and for the boundary values at $j = 0$ and $j = N$ the derivatives with respect to space x and time t should be approximated with forward (or backward) differences.

As stated in Section 4.4, we can choose any set of polynomial degrees in System (33). However, the existence of the system's solution (with respect to unknown polynomial coefficients) does not guarantee the stability of the mixed initial-boundary problem's (13) solution. ADTBCs could result in a partial reflection of outgoing waves back to the computational domain, solution's "explosion" (i.e. instability), or System (33) could not be solved for a given set of polynomial degrees (i.e. ADTBCs do not exist).

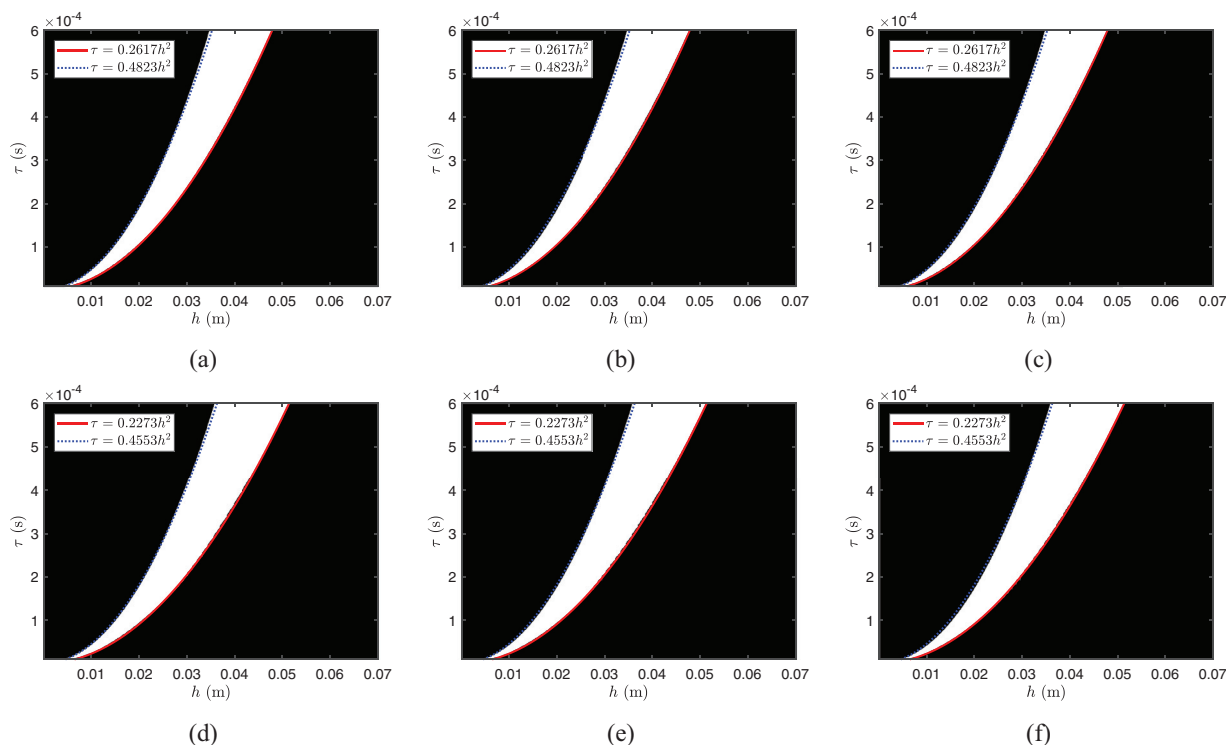


Fig. 1. The domain of stability on the (h, τ) plane for two ADTBCs. Left – energy norm criterion, centre – C-norm criterion, right – L^2 -norm criterion. The rows correspond to the particular set of polynomial degrees: (a), (b), (c) – $\langle 4, 4, 8, 8 \rangle$; (d), (e), (f) – $\langle 5, 3, 9, 7 \rangle$. The white area – stable, conditions (41), (42) and (43) are fulfilled (energy, C and L^2 norms, respectively). The black area – stability conditions are not fulfilled. Physical parameters of the rod ρ , E , R and L are the same as in Table 1.

If the set of polynomial coefficients does indeed provide the transparency of the border, then the corresponding solution should decrease over time. In fact, the waves spread outside of the computational domain, see Fig. 2. Therefore, we say that a finite-difference scheme with ADTBCs is stable, if at any time moment the energy norm of the solution obtained with these ADTBCs is less or equal to the energy norm at the initial time moment $t = 0$, i.e.

$$\sqrt{\hat{\mathcal{H}}[u^{n+1/2}]} \leq \sqrt{\hat{\mathcal{H}}[u^{1/2}]} \quad \forall n = 0, \dots, N_t - 1, \quad (41)$$

where we set the number of time steps to $N_t = 10^5$. Along with energy criterion (41) we introduce the classical stability criteria of C-norm

$$\|u^n\|_C \leq \|u^0\|_C, \quad \forall n = 0, \dots, N_t, \quad (42)$$

and L^2 -norm

$$\|u^n\|_{L^2} \leq \|u^0\|_{L^2}, \quad \forall n = 0, \dots, N_t. \quad (43)$$

The domains of stability (white) are presented in Fig. 1. For each case we approximate the boundaries between stable and unstable regions.

Unlike the classical equations of mathematical physics (wave, heat, Schrödinger equations), the classical stability criteria (42) and (43) for Eq. (12) are not necessarily fulfilled.

In our experiments for simplicity we used $U_1 \equiv 0$. For finite-difference Eq. (13) all these criteria are similar, see Fig. 1. There are small differences between all norms that occur near the boundaries between white and black regions. However, the approximation parabolas remain unchanged throughout all criteria, see Fig. 1a, 1 b, 1 c (Fig. 1d, 1 e, 1 f).

We denote the symbol of ADTBCs obtained with polynomial degrees $\text{deg}P_k = d_{1,k}$, $\text{deg}Q_k = d_{2,k}$, $\text{deg}R_k = d_{3,k}$ and $\text{deg}S_k = d_{4,k}$ with $k = 1, 2$ as

$$(P_k, Q_k, R_k, S_k) \equiv (d_{1,k}, d_{2,k}, d_{3,k}, d_{4,k}).$$

Eq. (12) on the segment $[-L/2, L/2]$ could be rewritten as

$$\frac{\partial^2 u}{\partial t^2} - D \frac{\partial^4 u}{\partial t^2 \partial x^2} + C \frac{\partial^4 u}{\partial x^4} = 0, \quad (44)$$

where the physical dimensions of the constants L , $D = R^2$, and $C = ER^2 \rho^{-1}$ are m, m^2 , and $\text{m}^4 \text{s}^{-2}$, respectively.

Usually, the stability condition of a finite-difference scheme of the Eq. (13) type has the form $\tau < Ah^2$, where the constant A has the physical dimension $m^{-2}s$ and depends on physical parameters and boundary conditions. Here, the time dimension is present only in the constant $C = ER^2\rho^{-1}$. Dimensionless parameter can be obtained only as a function of $\omega = L/R$. Therefore, from the dimension theory [43], it follows that $A = B(\omega)C^{-1/2}$.

From our numerical experiments, surprisingly, the time step τ should be bounded from both sides, which does not contradict the dimension theory. Moreover, the stability domain could be composed from several parabolic sectors:

$$A_1 h^2 < \tau < A_2 h^2,$$

where both constants could be expressed as

$$A_1 = B_1(\omega)C^{-1/2}, \quad A_2 = B_2(\omega)C^{-1/2}, \quad \omega = R/L,$$

with B_1 and B_2 being dimensionless functions depending also on the approximation scheme and on the type of boundary conditions (see Fig. 1). Our numerical experiments confirmed these statements and found no more than one of such sector on the (h, τ) plane.

5. Results of numerical experiments

5.1. Rod and scheme parameters, initial conditions, and reference solution

For our experiments we choose rod parameters that are similar to steel: $\rho = 7860 \text{ kg m}^{-3}$, $E = 210 \times 10^9 \text{ Pa}$. The radius of the rod is $R = 10^{-3} \text{ m}$. Therefore, $C = ER^2\rho^{-1} \approx 26.717557 \text{ m}^4 \text{ s}^{-2}$ and $D = R^2 = 10^{-6} \text{ m}^2$. The length of the rod is $L = 1 \text{ m}$, and $\omega = R/L = 10^{-3}$. We set the integration time to $T = 0.3 \text{ s}$. The point (h, τ) is located in the white areas of Fig. 1.

There is an infinite set of such ADTBCs gauges that could be obtained by solving System (36) and System (37). The obtained coefficients depend on all parameters of the model. Further we consider several sets of polynomial degrees used in ADTBCs construction Systems (33)–(35). Therefore, h and τ should be such that all boundary conditions would exist and not break the stability property.

We choose step h with respect to x to be equal to 0.02 m , and step τ with respect to t to be equal to $1.6 \times 10^{-4} \text{ s}$. In this case, dimensionless parameters are $\nu \approx 4.274809$ and $\mu = 0.0025$.

Note 13. The physical dimension of the solution is length. However, it may be multiplied by an arbitrary factor, since finite-difference Eq. (13) and ADTBCs (34) and (35) are linear. Therefore, the absolute values of the ordinate axis on all figures are optional.

We set initial conditions for Eq. (12) as

$$u(0, x) = \frac{x}{\sqrt{\pi \cdot 0.02}} \exp\left(-\frac{x^2}{0.02}\right), \quad \partial_t u(0, x) = 0, \quad x \in [-L/2, L/2]. \quad (45)$$

Therefore, for Eq. (13) we have initial conditions $u_0(x_i) = u(0, x_i)$, and $u_\tau(x_i) = u(\tau, x_i)$ is calculated using the algorithm proposed in Appendix E. The initial condition $u_0(x)$ is close to zero at the ends of the segment $[-L/2, L/2]$.

We define a reference solution $u^*(t, x)$ on the extended segment $[-40L, 40L]$, where we use the simplest (Dirichlet + Neumann) homogeneous boundary conditions. The initial rod's perturbation dissipates from the small segment. However, the plot in Fig. 2 confirms that the boundary conditions cannot significantly influence the solution at the segment $[-0.5L, 0.5L]$ during the integration period $t \in [0, 0.3]$.

The norms of the reference solution $u^*(t, x)$ decrease with time t as $x \in [-L/2, L/2]$, and the perfect DTBCs must provide the decrease of the corresponding norms of the difference between u^* and the solution of the mixed problem.

The dynamics of obtained solutions and the reference solution, as well as C-norm, are presented in online version in Appendix G.

Table 1
Values of parameters used in numerical simulations.

Parameter	Value	Dimension
ρ	7860	kg m^{-3}
E	210×10^9	Pa
R	10^{-3}	m
L	1	m
h	0.02	m
τ	1.6×10^{-4}	s
T	0.3	s
ν	≈ 4.274809	–
μ	0.0025	–

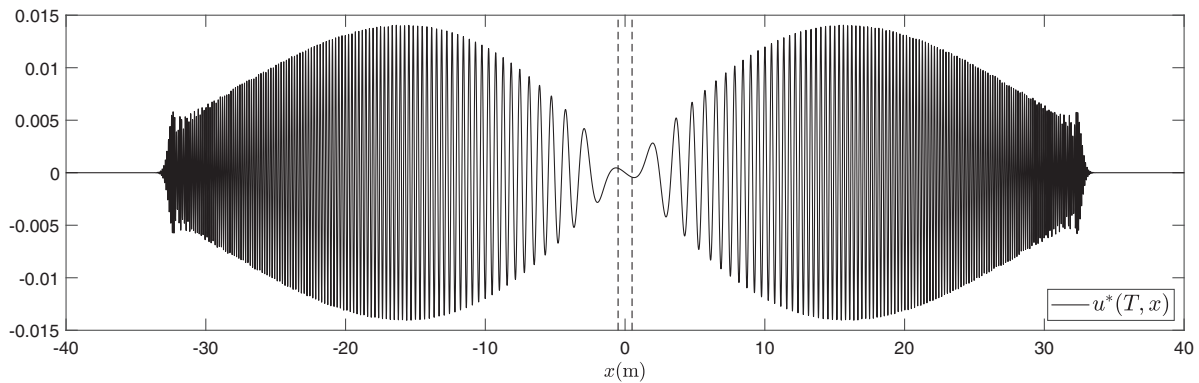


Fig. 2. The reference solution u^* on the very extended segment $[-40L, 40L]$ with initial conditions (45) at the final time moment $T = 0.3$. Two vertical dash lines indicate the borders of the considered segment $x \in [-L/2, L/2]$.

Table 2

The coefficients of the ADTBCs are obtained from Eqs. (34) and (35) for the sets of polynomial degrees $\langle P_k, Q_k, R_k, S_k \rangle = \langle 4, 4, 8, 8 \rangle$ at $k = 1, 2$.

	P_1	Q_1	R_1	S_1	P_2	Q_2	R_2	S_2
1	1	0	-0.555979	0.278657	0	1	-0.925737	0.301010
ω	-1.039354	-1.064260	0.925512	-0.300505	-0.039239	-1.498177	0.962232	-0.272787
ω^2	1.040798	0.175892	-0.343658	0.205584	-0.057023	1.346122	-0.918314	0.289728
ω^3	-0.484423	-0.688193	1.007943	-0.361839	0.240692	-1.187154	0.993006	-0.295379
ω^4	0.217631	-0.187829	0.258996	-0.095354	-0.007746	0.054903	0.027530	-0.020261
ω^5			0.101158	-0.063710			0.039188	-0.023854
ω^6			0.008250	-0.016540			0.004642	-0.006821
ω^7			-0.014938	0.002764			-0.005037	0.000709
ω^8			-0.005839	0.002373			-0.002124	0.000827

5.2. Basic version of transparent boundary conditions

There is an infinite set of choices of the degrees of polynomials $\langle P_1, Q_1, R_1, S_1 \rangle$ and $\langle P_2, Q_2, R_2, S_2 \rangle$, and therefore, an infinite number of corresponding ADTBCs. Moreover, it is essential to check the solvability of System (36) and System (37). If at least one of the systems does not have a unique solution for some set of polynomial degrees, then we cannot construct the ADTBCs for this set of degrees.

When the rational approximation in System (33) is performed, the stability of the Crank – Nicolson scheme might be lost. Therefore, one should account for solvability of System (36) and System (37), and check that the stability of the mixed problem is preserved. If the ADTBCs exist for the specific model's parameters and polynomial degrees, we apply them in computations and check if the result remains stable. Rational approximations (36) and (37) with finite polynomial degrees do not guarantee obtaining completely transparent boundaries. To determine if ADTBCs are reasonable, we investigate the error of the obtained solution u by comparing it to the reference solution u^* .

System (36) for $k = 1$, and System (37) for $k = 2$ consist of two similar equations for real and imaginary parts with the smallness order K . We also have two normalisation conditions on coefficients. Thus, the total number of unknown coefficients of these four polynomials that we have determined from System (36), as well as System (37), should be even.

As an example, let us consider the set of polynomial degrees

$$\deg P_k = \deg Q_k = 4, \deg R_k = \deg S_k = 8, \quad k = 1, 2. \quad (46)$$

Here and further we consider equal sets of polynomial degrees of boundary conditions for both border ($k = 1$) and pre-border ($k = 2$) points. The coefficients that correspond to the solutions of System (36) and System (37) for degree sets (46) are presented in Table 2.

Note 14. We provide values in the tables up to 6 decimal places. Our numerical experiments showed that by using the ADTBC coefficients without the 6-th decimal place the error increases just slightly, whereas without the 5th decimal place the increase is significant.

To evaluate the dynamics of the error of the obtained solution u of Eq. (13) with ADTBCs, we use the common logarithm (base 10) of three norms:

a) common logarithm of the Hamiltonian approximation $\hat{\mathcal{H}}$ of solutions' difference:

$$\log_{10} \sqrt{\hat{\mathcal{H}}[u(t, x) - u^*(t, x)]},$$

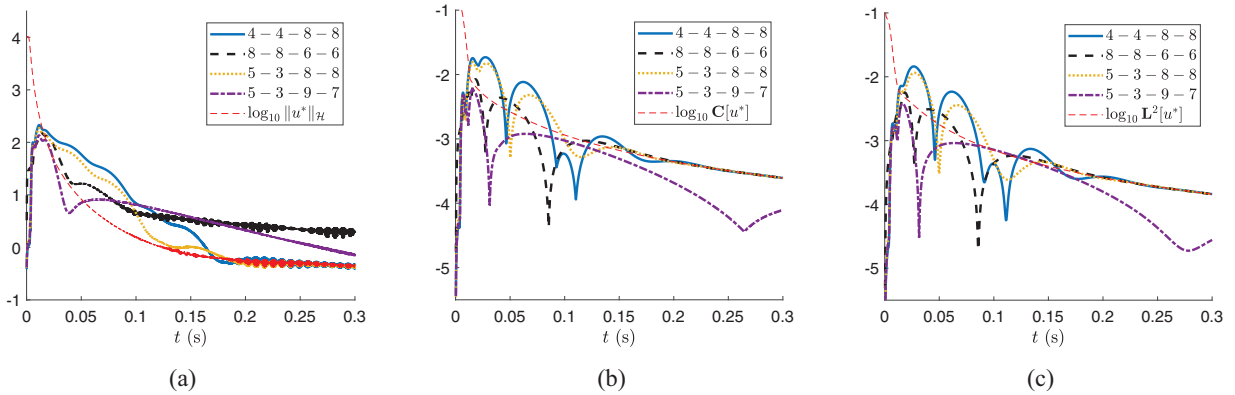


Fig. 3. Solid, thick dashed, dotted and dash-dotted lines represent common logarithm of (a) \hat{H} , (b) C-norm, (c) L^2 -norm of the difference between the reference solution u^* and solutions with ADTBCs. The narrow dashed line is common logarithm of (a) \hat{H} , (b) C-norm, (c) L^2 -norm of the reference solution u^* . Initial conditions are defined by formula (45).

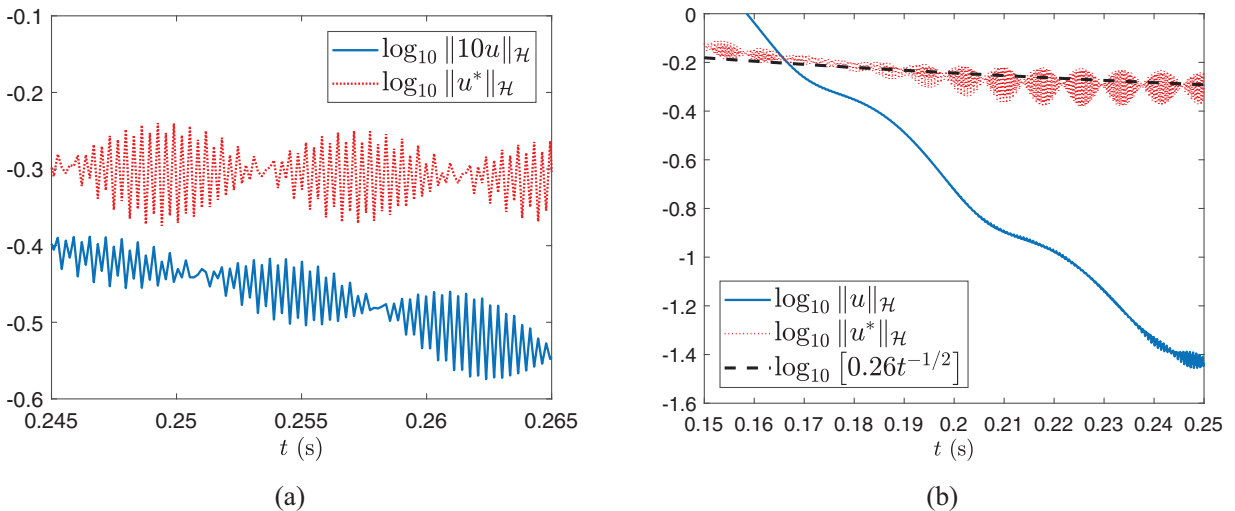


Fig. 4. (a) Common logarithm of \hat{H} of (solid line) the solution (multiplied by 10) obtained with ADTBCs with polynomial degrees $\langle 4, 4, 8, 8 \rangle$ and (dot line) the reference solution u^* on time interval $t \in [0.245, 0.265]$. (b) The decrease of energy in the period when most of it left the small segment, but has not yet reached the edges of the large segment. The dash line shows the asymptotic of the reference solution. Initial conditions are defined by formula (45).

b) common logarithm of the Chebyshev norm $C[-L/2, L/2]$ of solutions' difference, i.e.

$$\log_{10} \left[\max_{j=0,1,\dots,N} |u(t, x_j) - u^*(t, x_j)| \right],$$

c) common logarithm of L^2 -norm of solution's deference

$$\log_{10} [\|u(t, x) - u^*(t, x)\|_2],$$

where $\|u(t, x) - u^*(t, x)\|_2^2 = \int_{-L/2}^{L/2} (u(t, x) - u^*(t, x))^2 dx$, which is approximated by the standard trapezoidal method.

The results of our numeric experiments with different ADTBCs sets are presented in Fig. 3.

From Fig. 3a it follows that a part of the energy of the reference solution decreases approximately 20 000 times compared to the initial moment, because waves go away from the small segment. However, $\hat{H}(t)$ decreases slowly and non-monotonically when $t \rightarrow \infty$, see Fig. 4a, where the zoomed in fragment shows the dynamics of $\hat{H}(t)$ at $t \approx 0.25$. The oscillation of this functional occurs over time, the difference between two local maxima on the plot is equal to 2τ . The amplitude of the oscillations decreases very slowly, see Fig. 4b.

Note 15. Let us assume that at large times t , the oscillation energy is distributed almost uniformly over a segment and expands at about a constant speed on the straight line $x \in \mathbb{R}$. Then the energy that is concentrated on the segment $[-L/2, L/2]$ should decrease approximately as $O(t^{-1})$, and the energy norm of the solution as $O(t^{-1/2})$. Our evaluation shows that for this initial condition, the energy norm at $t \rightarrow \infty$ is estimated asymptotically as $0.26 \cdot t^{-1/2}$, see Fig. 4b.

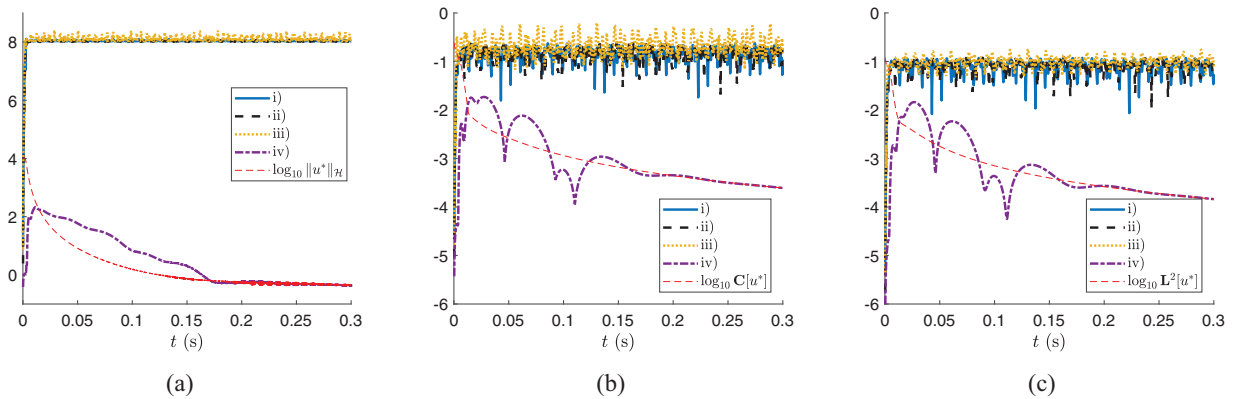


Fig. 5. The dashed, dotted and dash-dotted lines represent common logarithm of (a) \hat{H}_1 , (b) C -norm and (c) L^2 -norm of the difference between reference solution u^* and solution with 'usual' boundary conditions. The narrow dash line is common logarithm of (a) \hat{H}_1 , (b) C -norm and (c) L^2 -norm of the reference solution u^* . Initial conditions are defined by formula (45).

However, the ADTBCs with polynomial degrees $\langle 4, 4, 8, 8 \rangle$, as shown on Fig. 4, significantly reduce the part of the energy on the segment $[-L/2, L/2]$ in comparison to the reference solution. The difference of these energy norms is so significant that we needed to multiply the ADTBCs solution by 10 to place it in Fig. 4a.

Note 16. Also, we found that if the initial function $u_0 \equiv u(0, x)$ satisfy the Eq. (F3), then we can set additional requirements on the coefficients in Systems (36) and (37), which may reduce the error even further. However, the motivation behind this modification of DTBCs and ADTBCs does not have a physical interpretation, and the resulting error is not necessarily lower than in the standard method (described in Subsect. 4.4). We present the modification and results in Appendix F.

5.3. Comparison of transparent boundary conditions with various versions of 'Usual' homogeneous ones

In practice, simple homogeneous boundary conditions (i.e. Dirichlet and Neumann) are usually used when there is no information about physical processes on the border. These conditions lead to the partial or complete reflection of outgoing waves, back into the computational domain (sometimes with increased amplitude). On the contrary, ADTBCs that are calculated using our vectorial rational approximation techniques have a low reflection level.

Fig. 5 shows the dynamics of solutions' errors that are calculated using various 'usual' boundary conditions:

- i) $u|_{\Gamma} = 0, \frac{\partial u}{\partial x}|_{\Gamma} = 0 \Rightarrow u_0^n = u_1^n = 0,$
- ii) $u|_{\Gamma} = 0, \frac{\partial^2 u}{\partial x^2}|_{\Gamma} = 0 \Rightarrow u_0^n = 0, u_1^n = u_2^n/2,$
- iii) $\frac{\partial^2 u}{\partial x^2}|_{\Gamma} = 0, \frac{\partial^3 u}{\partial x^3}|_{\Gamma} = 0 \Rightarrow u_0^n = 3u_2^n - 2u_3^n, u_1^n = 2u_2^n - u_3^n,$
- iv) ADTBCs with polynomial degrees $\langle P_k, Q_k, R_k, S_k \rangle = \langle 4, 4, 8, 8 \rangle, k = 1, 2.$

All these homogeneous boundary conditions i) - iii) lead to a significant reflection of outgoing waves back into the computational area, see Fig. 5. The obtained solutions almost immediately differ from the reference solution, whereas the solution obtained with ADTBCs (iv) stays close to u^* during the integration time.

The smoothed evolution of the solution with ADTBCs (with degrees $\langle 4, 4, 8, 8 \rangle$) is shown in Fig. 6. Lines where $|u(t, x) - u^*(t, x)| = 0$ are generally not visible, except in the middle of the segment, where both solutions are small, because they are odd for all t . Fig. 6 shows that for large t , the difference $|u(t, x) - u^*(t, x)|$ is slowly decreasing. According to Fig. 4, it is because the reference solution slowly decreases, but the solution with ADTBCs at this time is orders of magnitude less.

6. Discussion

ADTBCs might be used in the mathematical modelling of processes on a finite area, when it is certain that external processes do not have any essential impact on the interior. On the other hand, ADTBCs could suspend all fluctuations in the finite area without using any high computational viscosity on some borders' vicinity.

The problem of constructing transparent conditions becomes more complex if the coefficients of the partial differential (or finite-difference) equation are variable, and/or the bounded computational domain V has a sophisticated boundary. In such cases, it is usually not possible to apply the method of separation of independent variables. In [38], for the anisotropic elasticity, it is proposed to generalise the approach [44] of fast analytical TBC for the wave equation to the case of variable coefficients. The quasi-analytical ADTBC operator [38] is generated numerically and its accuracy depends on the number of basis functions representing the solution at the open boundary. The problem of arbitrary computational domain can be solved by immersion into a sphere with ADTBC using domain decomposition conception as proposed in [45]. In the works

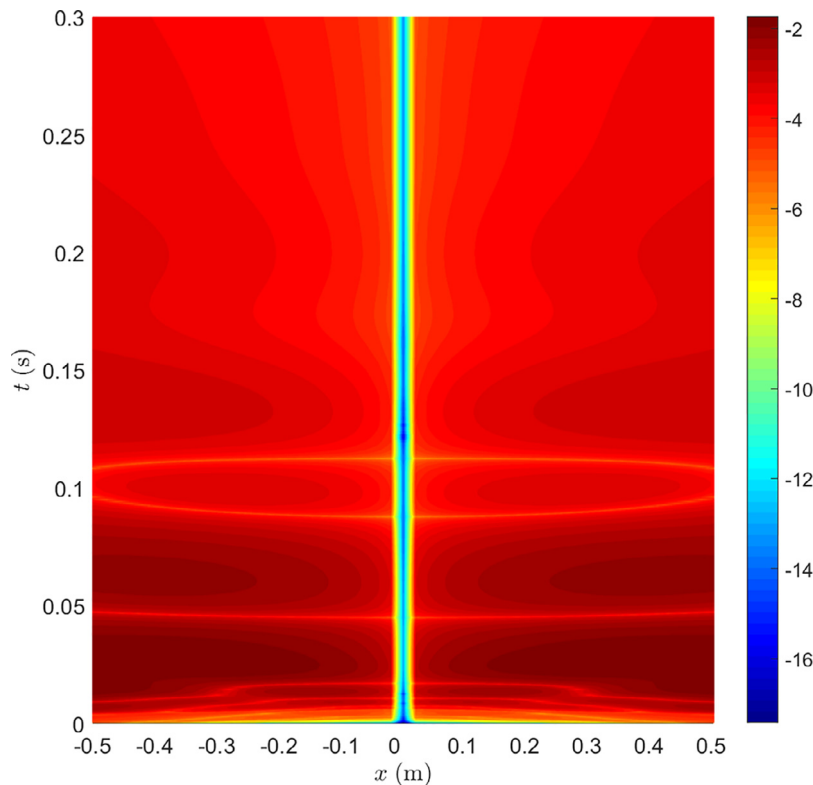


Fig. 6. Common logarithm of absolute difference between reference solution u^* and the mixed problem solution with ADTBCs with polynomial degrees $\langle P_k, Q_k, R_k, S_k \rangle = \langle 4, 4, 8, 8 \rangle$, $k = 1, 2$ at different time moments t . Initial conditions are defined by formula (45).

[8–12,14,18,19,21,22] (and also in this article), only problems where the variable separation is possible were considered. On the other hand, here the construction of DTBCs and ADTBCs for the difference problem is performed directly and not by means of a difference approximation of the boundary operators for the differential problem.

In our work we propose the algorithm of determining ADTBCs operators, which can be done for fixed parameters of the rod and time-space steps. However, if the parameters or pair (h, τ) are changed, a numerical recalculation is needed. For the Schrödinger equation to recalculate DTBC operators for other pairs (h, τ) a transformation rule was proposed by using one and the same rational approximation, see [17].

A characteristic feature of DTBCs is non-locality with respect to time. Values of the solution in the vicinity of a border at previous time steps are required. We used a vectorial rational approximation generalising the Hermite – Padé approximation. It allows us to reduce this number of time steps in the convolutions. In spatially multidimensional finite-difference models, where the corresponding DTBCs are non-local with respect to variables that are tangential to the area's boundary, vectorial rational approximation can also be applied, which would significantly reduce computational costs, see [8–11,13–20,22,38,44].

7. Conclusion

In this paper, we have constructed Approximate Discrete Transparent Boundary Conditions (ADTBCs) for the implicit finite-difference scheme that approximates the fourth order differential equation with respect to space. Both equations (differential and finite-difference) require two boundary conditions on each end. The considered differential equation is more sophisticated than many classic mathematical physics equations, because it is not resolved with respect to the highest derivative of a solution with respect to time (i.e. it does not belong to Cauchy – Kovalevskaya type).

Here, the ADTBCs were constructed for the finite-difference Crank – Nicolson implicit scheme for the transverse vibrations equation of a rod (beam) with a circular cross section. ADTBCs provide a solution of a mixed initial-boundary value problem on a segment that is close to the solution on the infinite domain.

We proved the absolute stability of the Crank – Nicolson scheme for the Cauchy problem, and experimentally verified the conditional stability of the mixed boundary value problem with ADTBCs. It is shown that the stability regions depend on the rational approximation (i.e. sets of polynomial degrees), and are bound by two parabolas on the (h, τ) plane.

It is shown that 'usual' (Dirichlet and Neumann) homogeneous boundary conditions do not have this 'transparency' property. The need of such ADTBCs is seen in many scientific and technical applications. The approach may be applied, when

we need to imitate a non-zeroth background solution (at a large area) and a forcing f . In these cases ADTBCs will be non-homogeneous.

All DTBCs and ADTBCs derived here, are characterised by lots of numerical parameters (physical parameters of a rod, degrees of approximating polynomials in System (33), space h and time τ steps). Resulting ADTBCs should be defined with at least five decimal places. We describe the algorithm of parameter determination (symbolic computations were used), which is the main result of this paper.

The proposed algorithms of ADTBCs construction can be used for various evolutionary linear equations or systems and their finite-difference approximations. However, recalculations of all coefficients and formulae derivations for the ADTBCs are required, if other finite-difference approximation schemes are used.

We also present the algorithm (based on the compact finite-difference scheme) of the initial functions calculation that provides a high-order of approximation with respect to time, for the implicit finite-difference equation.

Acknowledgments

We are cordially grateful to Ph. L. Bykov for useful discussions in the course of our work. We are very grateful to anonymous reviewers, whose comments helped us to correct inaccuracies, confusions and deficiencies.

The article was prepared within the framework of the Academic Fund Program at HSE University in 2018 – 2019 (grant № 18-05-0011), in 2020 – 2021 (grant № 20-04-021) and within the framework of the Russian Academic Excellence Project “5-100”.

Appendix A. Expansion of Functions $\eta_{1,2}(\omega)$ into Taylor Series

We represent the radicand in Eq. (22) with a help of dimensionless parameters ν and μ and simplify it:

$$\eta_1(\omega) = \frac{-\beta(1+\omega^2) - \gamma\omega - \sqrt{(1-\omega)^2[(\mu^2-2\nu)\omega^2 - 2\mu^2\omega + \mu^2 - 2\nu]}}{2\sigma(1+\omega^2)}.$$

If $|\omega| < 1$, we can take out the multiplier from the quadratic root:

$$\eta_1(\omega) = \frac{-\beta(1+\omega^2) - \gamma\omega - \sqrt{\mu^2 - 2\nu}(1-\omega)\sqrt{\omega^2 - 2\frac{\mu^2}{\mu^2-2\nu}\omega + 1}}{2\sigma(1+\omega^2)}.$$

Let us apply the formula for the generating function of the Legendre polynomials (see e.g. [14,16,18,20,22,46–48]):

$$(\omega^2 - 2\varepsilon\omega + 1)^{-1/2} = \sum_{n=0}^{\infty} P_n(\varepsilon)\omega^n,$$

where $P_n(\varepsilon)$ is the Legendre polynomial of degree n at point ε . Here $\varepsilon = \frac{\mu^2}{\mu^2-2\nu}$, $|\varepsilon| < 1$. We obtain

$$\eta_1(\omega) = \frac{1}{2\sigma(1+\omega^2)} \left[-\beta(1+\omega^2) - \gamma\omega - \sqrt{\mu^2 - 2\nu}(1-\omega) \left(\omega^2 - 2\frac{\mu^2}{\mu^2-2\nu}\omega + 1 \right) \sum_{n=0}^{\infty} P_n\left(\frac{\mu^2}{\mu^2-2\nu}\right)\omega^n \right].$$

Then we use the formula for geometric progression:

$$\frac{1}{1+a} = \sum_{k=0}^{\infty} (-1)^k a^k,$$

where $a = \omega^2$, and express values β, γ, δ across μ and ν . We obtain:

$$\eta_1(\omega) = \frac{1}{\nu} \sum_{k=0}^{\infty} (-1)^k \omega^{2k} \cdot \left[(\mu + 2\nu)(1+\omega^2) - 2\mu\omega - \sqrt{\mu^2 - 2\nu}(1-\omega) \left(\omega^2 - 2\frac{\mu^2}{\mu^2-2\nu}\omega + 1 \right) \sum_{n=0}^{\infty} P_n\left(\frac{\mu^2}{\mu^2-2\nu}\right)\omega^n \right]. \quad (\text{A.1})$$

In the same way we obtain

$$\eta_2(\omega) = \frac{1}{\nu} \sum_{k=0}^{\infty} (-1)^k \omega^{2k} \cdot \left[(\mu + 2\nu)(1+\omega^2) - 2\mu\omega + \sqrt{\mu^2 - 2\nu}(1-\omega) \left(\omega^2 - 2\frac{\mu^2}{\mu^2-2\nu}\omega + 1 \right) \sum_{n=0}^{\infty} P_n\left(\frac{\mu^2}{\mu^2-2\nu}\right)\omega^n \right]. \quad (\text{A.2})$$

Appendix B. Expansion of Functions $\lambda_i(\omega)$, $i = 1, \dots, 4$ into Taylor Series

We can rewrite the functions $\lambda_{1,3}(\omega)$ in the form

$$\lambda_{1,3}(\omega) = \frac{\eta_1(\omega)}{2} \mp \sqrt{\frac{1}{4}(\vartheta_1 + r_1(\omega))^2 - 1},$$

and factor the radicand:

$$\lambda_{1,3}(\omega) = \frac{\eta_1(\omega)}{2} \mp \sqrt{\left(\frac{\vartheta_1 + r_1(\omega)}{2} + 1\right) \cdot \left(\frac{\vartheta_1 + r_1(\omega)}{2} - 1\right)}.$$

Then we represent the radicand as a product

$$\lambda_{1,3}(\omega) = \frac{\eta_1(\omega)}{2} \mp \sqrt{\frac{\vartheta_1^2}{4} - 1} \cdot \sqrt{1 + \frac{r_1(\omega)}{\vartheta_1 + 2}} \cdot \sqrt{1 + \frac{r_1(\omega)}{\vartheta_1 - 2}},$$

and use the formula for the Taylor series expansion of a square root:

$$\sqrt{1+x} = \sum_{n=0}^{\infty} \frac{(-1)^n (2n)!}{(1-2n)n! 4^n} x^n, \quad |x| < 1,$$

to obtain the Taylor series for the characteristic roots in the vicinity of $\omega = 0$

$$\lambda_{1,3}(\omega) = \frac{\eta_1(\omega)}{2} \mp \sqrt{\frac{\vartheta_1^2}{4} - 1} \cdot \sum_{n=0}^{\infty} \frac{(-1)^n (2n)! r_1^n(\omega)}{(1-2n)n! 4^n (\vartheta_1 + 2)^n} \cdot \sum_{n=0}^{\infty} \frac{(-1)^n (2n)! r_1^n(\omega)}{(1-2n)n! 4^n (\vartheta_1 - 2)^n}, \quad (\text{B.1})$$

where $\eta_1(\omega)$ and $r_1(\omega)$ are taken from Eqs. (23) and (25), respectively.

In the same way we obtain the Taylor series expansion for other characteristic roots:

$$\lambda_{2,4}(\omega) = \frac{\eta_2(\omega)}{2} \mp \sqrt{\frac{\vartheta_2^2}{4} - 1} \cdot \sum_{n=0}^{\infty} \frac{(-1)^n (2n)! r_2^n(\omega)}{(1-2n)n! 4^n (\vartheta_2 + 2)^n} \cdot \sum_{n=0}^{\infty} \frac{(-1)^n (2n)! r_2^n(\omega)}{(1-2n)n! 4^n (\vartheta_2 - 2)^n}, \quad (\text{B.2})$$

where functions $\eta_2(\omega)$ and $r_2(\omega)$ are taken from Eqs. (24) and (25), respectively.

Appendix C. Legendre Polynomial Calculation

In our numerical experiments (in Subsect. 4.3 and Appendix A) we use coefficients of Taylor expansions of algebraic functions and their rational approximations (see [42]). Convergence of such series depends on the location of functions' singular points on the complex plane.

We need to calculate Legendre polynomials $P_n(\varepsilon)$ of order n in Eqs. (23), (24). It is necessary to assess the speed of decrease of $P_n(\varepsilon)$ with increasing order n . Asymptotic formula for $\varepsilon = \cos \alpha$ as $n \rightarrow \infty$ (see, e.g. [46,48])

$$P_n(\cos \alpha) = \sqrt{\frac{2}{\pi n \sin \alpha}} \sin(n\alpha + \alpha/2 + \pi/4) + \mathbf{O}(n^{-3/2}) \quad (\text{C.1})$$

holds for $|\varepsilon| < 1$. In our case, we need to make sure that the absolute value of Legendre polynomials' argument is less than one: $\left| \frac{\mu^2}{\mu^2 - 2\nu} \right| < 1$, which is true if $\mu^2 < \nu$. By definition, it leads to

$$\tau > \sqrt{\frac{R^2 \rho}{E}}.$$

Note that in our numerical experiment (see Subsect. 5.1) it corresponds to $\tau \approx 1.9346 \cdot 10^{-6}$ s. In some other examples the inequality $|\varepsilon| < 1$ coincides with the Courant stability condition of finite-difference scheme, see [14,19,22].

From Eq. (C.1) we see that the decrease of Legendre polynomial values is not fast. With increasing n the calculation of Legendre polynomials becomes a numerically difficult task. Standard recurrent formula at point ε

$$(n+1)P_{n+1}(\varepsilon) = (2n+1)\varepsilon P_n(\varepsilon) - nP_{n-1}(\varepsilon)$$

may accumulate a big error for high n . We use the approach proposed by Belousov (see [49,50]):

$$\begin{aligned} P_n(\cos \alpha) = & \sqrt{\frac{2n+1}{2}} \frac{1 \cdot 3 \cdot 5 \dots (2n-1)}{2^{n-1} \cdot n!} \left[\cos n\alpha + \frac{1}{1} \frac{n}{2n-1} \cos(n-2)\alpha + \right. \\ & \left. + \frac{1 \cdot 3}{1 \cdot 2} \frac{n(n-1)}{(2n-1)(2n-3)} \cos(n-4)\alpha + \right. \end{aligned}$$

$$\begin{aligned}
& + \frac{1 \cdot 3 \cdot 5}{1 \cdot 2 \cdot 3} \frac{n(n-1)(n-2)}{(2n-1)(2n-3)(2n-5)} \cos(n-6)\alpha + \dots \\
& \dots + \left[\begin{aligned} & \frac{(n-2)!!}{[n/2]!} \frac{\prod_{k=1}^{[n/2]} (n-k+1)}{\prod_{k=1}^{[n/2]} (2n-2k+1)} \cos \alpha \quad \text{if } n \text{ is odd,} \\ & \frac{1}{2} \cdot \frac{(n-2)!!}{(n/2)!} \frac{\prod_{k=1}^{n/2} (n-k+1)}{\prod_{k=1}^{n/2} (2n-2k+1)} \cos 0\alpha \quad \text{if } n \text{ is even} \end{aligned} \right]. \quad (C.2)
\end{aligned}$$

Here brackets $[\cdot]$ denote rounding down (floor function). The series in Eq. (C.2) conclude with a term containing $\cos \alpha$ with n being odd. If n is even, the series is concluded with a term containing $\cos 0\alpha$. The last coefficient (before $\cos 0\alpha$) is additionally multiplied by $1/2$.

Appendix D. Stability of the Crank – Nicolson approximation of the rod transverse vibrations equation

Here we investigate the stability of Crank – Nicolson approximation of rod transverse vibrations equation on infinite domain, i.e. without boundary conditions. After the Fourier transform of Eq. (13)

$$\sigma(u_{m+2}^{n+1} + u_{m-2}^{n+1} + u_{m+2}^{n-1} + u_{m-2}^{n-1}) + \beta(u_{m+1}^{n+1} + u_{m-1}^{n+1} + u_{m+1}^{n-1} + u_{m-1}^{n-1}) + \alpha(u_m^{n+1} + u_m^{n-1}) + \gamma(u_{m-1}^n + u_{m+1}^n) + \delta u_m^n = 0$$

we get the ordinary finite-difference equation

$$\sigma[2 \cos(2\xi h)(w^{n+1} + w^{n-1})] + \beta[2 \cos(\xi h)(w^{n+1} + w^{n-1})] + \alpha(w^{n+1} + w^{n-1}) + [2\gamma \cos(\xi h) + \delta]w^n = 0, \quad (D.1)$$

where ξ is dual to spatial variable, w is the solutions's image.

The equation for the next time step has the matrix form

$$\begin{pmatrix} w^{n+1} \\ w^n \end{pmatrix} = \begin{pmatrix} -\frac{2\gamma \cos(\xi h) + \delta}{2\sigma \cos(2\xi h) + 2\beta \cos(\xi h) + \alpha} & -1 \\ 1 & 0 \end{pmatrix} \begin{pmatrix} w^n \\ w^{n-1} \end{pmatrix}. \quad (D.2)$$

Simplifying Eq. (D.2) we get

$$\begin{pmatrix} w^{n+1} \\ w^n \end{pmatrix} = \begin{pmatrix} -\frac{4\mu \cos(\xi h) - 2 - 4\mu}{2\nu \cos^2(\xi h) - 2(2\nu + \mu) \cos(\xi h) + 1 + 2\nu + 2\mu} & -1 \\ 1 & 0 \end{pmatrix} \begin{pmatrix} w^n \\ w^{n-1} \end{pmatrix}. \quad (D.3)$$

For Scheme (13) to be stable, it is necessary for the largest absolute value of the eigenvalue of matrix in Eq. (D.3) to be less or equal to one for any real ξ :

$$\max_{i=1,2} |\text{eig}_i(\xi)| \leq 1, \quad \forall \xi \in \mathbb{R}. \quad (D.4)$$

According to Vieta's theorem for characteristic equation for matrix in Eq. (D.3), the product of both eigenvalues is equal to one. Therefore, the stability is obtained when the discriminant of the corresponding characteristic equation is non-positive:

$$\left(\frac{2\mu \cos(\xi h) - 1 - 2\mu}{2\nu \cos^2(\xi h) - 2(2\nu + \mu) \cos(\xi h) + 1 + 2\nu + 2\mu} \right)^2 - 1 \leq 0. \quad (D.5)$$

The numerator in the parentheses in Eq. (D.5) is negative for any ξ :

$$2\mu(\cos(\xi h) - 1) - 1 < 0. \quad (D.6)$$

The denominator in parentheses in Eq. (D.5) can be rewritten as

$$2\nu(1 - \cos(\xi h))^2 + 2\mu(1 - \cos(\xi h)) + 1 > 0 \quad \forall \xi \in \mathbb{R}. \quad (D.7)$$

Therefore, the stability condition Eq. (D.5) becomes

$$-2\mu(\cos(\xi h) - 1) + 1 \leq 2\nu(1 - \cos(\xi h))^2 + 2\mu(1 - \cos(\xi h)) + 1,$$

or simply

$$2\nu(1 - \cos(\xi h))^2 \geq 0, \quad (D.8)$$

which is true for any real ξ . Hence, the approximation is absolutely stable.

Appendix E. Initial data construction

Let us decompose solution $u(t, x)$ into a Taylor series with respect to time in the vicinity of $t = 0$:

$$u(\tau, x) = U_0(x) + U_1(x)\tau + U_2(x)\frac{\tau^2}{2!} + \dots, \quad (E.1)$$

where $U_k(x) = \frac{\partial^k u}{\partial t^k}(0, x)$. The functions U_0, U_1 compose initial conditions for Eq. (1). To determine the left hand side in Eq. (E.1) with an error $O(\tau^3)$, we need to compute the function U_2 .

Table E1

The pairs of test functions and the corresponding linear algebraic equations for coefficients of compact finite-difference scheme (E.4).

No	u_k	f_k	Algebraic equation for the coefficients of Eq. (E.4)
0	0	1	$2p + 2q + r = 0$
1	0	$(x - x_j)^2$	$8p + 2q = 0$
2	$-24C$	$(x - x_j)^4$	$-24C(2a + 1) = (32p + 2q)h^4$
3	$-360C((x - x_j)^2 + 2D)$	$(x - x_j)^6$	$-720DC(2a + 1) - 720Cah^2 = 2p(2h)^6 + 2qh^6$

We differentiate Eq. (E.1)

$$\begin{aligned}\frac{\partial^2 u}{\partial \tau^2}(\tau, x) &= \sum_{k=2}^{\infty} U_k(x) \frac{\tau^{k-2}}{(k-2)!}, \\ \frac{\partial^4 u}{\partial \tau^2 \partial x^2}(\tau, x) &= \sum_{k=2}^{\infty} U_k''(x) \frac{\tau^{k-2}}{(k-2)!}, \\ \frac{\partial^4 u}{\partial x^4}(\tau, x) &= \sum_{k=2}^{\infty} U_k^{[iv]}(x) \frac{\tau^k}{k!},\end{aligned}$$

and substitute the series into Eq. (12):

$$\sum_{k=2}^{\infty} U_k(x) \frac{\tau^{k-2}}{(k-2)!} - R^2 \sum_{k=2}^{\infty} U_k''(x) \frac{\tau^{k-2}}{(k-2)!} + \frac{ER^2}{\rho} \sum_{k=0}^{\infty} U_k^{[iv]}(x) \frac{\tau^k}{k!} = 0.$$

Collecting similar terms at the zeroth degree of τ we obtain the following linear ordinary differential equation for U_2 with constant coefficients:

$$\left[D \frac{d^2}{dx^2} - 1 \right] U_2(x) = C U_0^{[iv]}(x), \quad (E.2)$$

where $D = R^2$ and $C = ER^2 \rho^{-1}$.

We assume here that both initial function $U_0^{[iv]}(x)$ and auxiliary function $U_2(x)$ are rapidly decreasing at infinity. In this case, the principal term of the asymptotic at infinity of the non-increasing solution of the non-homogeneous differential equation, can be determined from the homogeneous one:

$$U_2(x) \sim \exp\left(\frac{-x}{\sqrt{D}}\right) \text{ as } x \rightarrow +\infty, \quad U_2(x) \sim \exp\left(\frac{x}{\sqrt{D}}\right) \text{ as } x \rightarrow -\infty. \quad (E.3)$$

We approximate Eq. (E.2) by a compact finite-difference scheme (for details see, e.g. [16,51]):

$$\begin{aligned}aU_2(x_{j-1}) + U_2(x_j) + aU_2(x_{j+1}) &= pU_0(x_{j-2}) + qU_0(x_{j-1}) + rU_0(x_j) + qU_0(x_{j+1}) + pU_0(x_{j+2}), \\ j &\in [-J+1, J-1].\end{aligned} \quad (E.4)$$

To determine the unknown four values a, p, q, r we substitute into Eq. (E.4) four pairs of the test functions $\langle U_{2,k}, U_{0,k} \rangle \equiv \langle u_k, f_k \rangle$, $k = 0, 1, 2, 3$, which satisfy Eq. (E.2) and are listed in Table E.3.

Differential Eq. (E.2) and finite-difference Eq. (E.4) both include only even order operators with constant coefficients. Therefore, the following odd test functions $\langle u, f \rangle$ like $\langle 0, (x - x_j) \rangle$ or $\langle (x - x_j)^{2m+1}, D \cdot (2m+1) \cdot 2m \cdot (x - x_j)^{2m-1} - (x - x_j)^{2m+1} \rangle$ satisfy Eq. (E.4) for any coefficients. That is why only even test functions are used for the approximation.

Solution of the system of these four linear algebraic equations is

$$a = \frac{h^2 - 6D}{12D + 4h^2}, \quad p = \frac{-3C}{2h^2(3D + h^2)}, \quad q = \frac{6C}{h^2(3D + h^2)}, \quad r = \frac{-9C}{h^2(3D + h^2)}.$$

Three-diagonal system of $2J - 1$ linear algebraic Eqs. (E.4) and the finite-difference approximations of formulae (E.3): $U_2(x_{-J}) = \exp(-h/\sqrt{D}) U_2(x_{-J+1})$ and $U_2(x_J) = \exp(-h/\sqrt{D}) U_2(x_{J-1})$ is closed and non-degenerate. It can be solved by the classical double-sweep method.

If it is necessary to increase the order of accuracy of the initial function $u(\tau, x)$, we should similarly define a function $U_3(x)$ and substitute it into Eq. (12), etc.

Appendix F. Possible modification of ADTBCs

The function $u(t, x) \equiv \text{const}$ is a solution of differential Eq. (12) and the finite-difference Eq. (13). We can additionally require the DTBCs and ADTBCs to satisfy this solution. In other words, we introduce an additional linear condition on the polynomial coefficients in System (36) and System (37) for $k = 1$ and for $k = 2$ (their total sums must be equal to zero):

$$P_k(1) + Q_k(1) + R_k(1) + S_k(1) = 0. \quad (F.1)$$

As mentioned in Subs. 5.1, an even number of unknown coefficients is required to construct the ADTBCs. To maintain the same approximation order of System (36) and System (37) with additional condition (F.1), one extra coefficient is required and, thus, the number of these coefficients becomes odd.

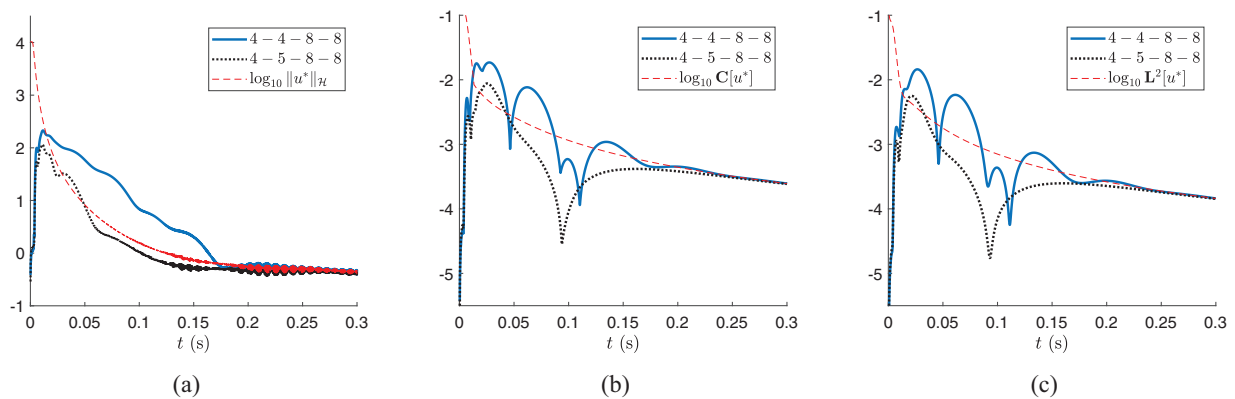


Fig. F1. Solid and dotted lines represent common logarithm of (a) \hat{H} , (b) C-norm, (c) L^2 -norm of the difference between the reference solution u^* and the solutions obtained with ADTBCs. The dotted line corresponds to the ADTBCs with additional requirement Eq. (F.1) taken into account in the polynomial coefficient calculation. The dash line stands for common logarithm of (a) \hat{H} , (b) C-norm, (c) L^2 -norm of the reference solution u^* . Initial conditions are defined by formula (45).

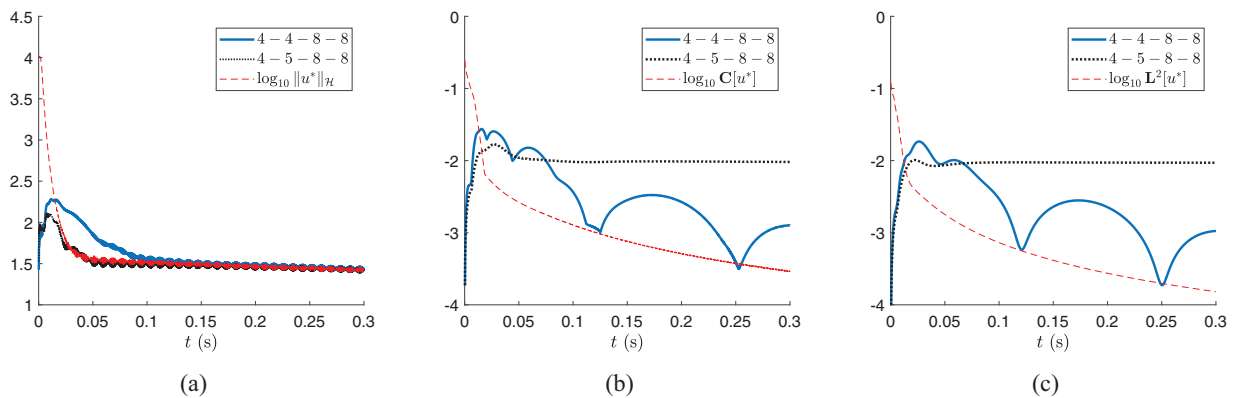


Fig. F2. Solid and dotted lines represent common logarithm of (a) \hat{H} , (b) C-norm, (c) L^2 -norm of the difference between the reference solution u^* and the solutions obtained with ADTBCs. The dotted line corresponds to the ADTBCs with additional requirement Eq. (F.1) taken into account in the polynomial coefficient calculation. The dash line is common logarithm of (a) \hat{H} , (b) C-norm, (c) L^2 -norm of the reference solution u^* . Initial conditions are defined by formula (F.4).

Table F1

The coefficients of the ADTBCs are obtained from Eqs. (34) and (35), and additional condition (F.1) for the sets of polynomial degrees $\langle P_k, Q_k, R_k, S_k \rangle = \langle 4, 5, 8, 8 \rangle$ at $k = 1, 2$.

	P_1	Q_1	R_1	S_1	P_2	Q_2	R_2	S_2
1	1	0	-0.555979	0.278657	0	1	-0.925737	0.301010
ω	-2.554692	2.432054	-1.468661	0.329664	-0.491692	-0.454239	0.247374	-0.084630
ω^2	2.067232	-1.792876	0.313255	0.091235	0.249452	0.758283	-0.722172	0.255585
ω^3	-2.170815	2.376252	-0.936209	0.136683	-0.262835	-0.272165	0.412516	-0.146529
ω^4	1.325085	-1.388514	0.900316	-0.202468	0.322920	-0.303600	0.219016	-0.052243
ω^5		-0.519196	0.545430	-0.195266		-0.155023	0.171840	-0.063135
ω^6			0.009158	-0.011746			0.004913	-0.005389
ω^7			-0.007229	0.000655			-0.002735	0.000079
ω^8			-0.003216	0.001191			-0.001341	0.000474

As a new example, we modify previous ADTBCs sets:

$$\deg P_k = 4, \deg Q_k = 5, \deg R_k = \deg S_k = 8, \quad k = 1, 2. \quad (\text{F.2})$$

The coefficients of these sets that are derived from System (36) and System (37) with additional condition (F.1) are presented in Table F.4.

The introduced modification of DTBCs and ADTBCs construction can only be applied when the initial function $U_0 \equiv u(0, x)$ has zeroth integral over the segment:

$$\int_{-L/2}^{L/2} u(0, x) dx = 0. \quad (\text{F.3})$$

When the condition (F.3) does not hold, the resulting ADTBCs do not provide the transparency property. In Fig. F.8, we present the errors for sets $\langle 4, 4, 8 \rangle$ and $\langle 4, 5, 8 \rangle$, and shifted initial conditions:

$$u(0, x) = \frac{(x - 0.1)}{\sqrt{\pi \cdot 0.02}} \cdot \exp\left(-\frac{(x - 0.1)^2}{0.02}\right), \quad \partial_t u(0, x) = 0, \quad x \in [-L/2, L/2]. \quad (\text{F.4})$$

Approximate solution's error under the ADTBCs (F.2) with additional requirement (F.1) is mostly smaller (see Fig. F.7). Therefore, the introduction of this condition on coefficients results in a decrease of the error for any time moment t , provided the initial conditions satisfy Eq. (F.3).

Appendix G. Dynamics of obtained solutions for different ADTBCs

Here we present animations of the obtained solutions u and the reference solution u^* (left). We also provide the common logarithm of C-norm of absolute difference between the two solutions (right).

Sets of polynomial degrees are denoted as $\text{deg}P_k - \text{deg}Q_k - \text{deg}R_k - \text{deg}S_k$ (being equal for $k = 1$ and $k = 2$) in the title of animations.

All results are obtained using the same parameters and initial conditions as in Subsect. 5.1.

Supplementary material

Supplementary material associated with this article can be found, in the online version, at doi:10.1016/j.apm.2020.06.050.

References

- [1] S. Timoshenko, *Vibration Problems in Engineering*, Read Books, 2008.
- [2] M.S. Agranovich, Boundary value problems for systems with a parameter, *Math. USSR-Sb.* 13 (1971) 25–64.
- [3] L. Hörmander, *The Analysis of Linear Partial Differential Operators III, Pseudo-Differential Operators*, Springer-Verlag, Berlin Heidelberg, 2007.
- [4] H.O. Kreiss, Initial boundary value problems for hyperbolic systems, *Commun. Pure Appl. Math.* 23 (1970) 277–298.
- [5] H.-O. Kreiss, H.U. Busenhardt, *Time-Dependent Partial Differential Equations and Their Numerical Solution*, Birkhäuser, 2001.
- [6] R. Sakamoto, Mixed problems for hyperbolic equations I energy inequalities, *J. Math. Kyoto Univ.* 10 (1970) 349–373.
- [7] R. Sakamoto, Mixed problems for hyperbolic equations II, existence theorem with zero initial data and energy inequalities with initial datas, *J. Math. Kyoto Univ.* 10 (1970) 403–417.
- [8] B. Engquist, A. Majda, Absorbing boundary conditions for numerical simulation of waves, *Proc. Natl. Acad. Sci.* 74 (1977) 1765–1766.
- [9] V.A. Gordin, Some mathematical problem of the numerical hydrodynamic forecasting, in: *Proceedings of the Lectures of Second Conferences of Young Scientists of the Hydrometeorological Service of USSR (in Russian)*, Obninsk, USSR, 1977, pp. 11–17.
- [10] B. Engquist, A. Majda, Radiation boundary conditions for acoustic and elastic wave calculations, *Commun. Pure Appl. Math.* 32 (1979) 313–357.
- [11] V.A. Gordin, On a mixed boundary-value problem imitating the cauchy problem, *Russ. Math. Surv.* 33 (1978) 189–190.
- [12] V.A. Gordin, *The Study of the Finite-Difference Approximations and Boundary Conditions for Systems of Forecasting Equations*, Hydrometeorological Center of the USSR, Moscow, 1979 Ph.D. thesis (in Russian).
- [13] V.A. Gordin, *Mathematical Problems of the Hydrodynamical Weather Forecasting. Analytic Aspects (in Russian)*, Gidrometeoizdat, Leningrad, USSR, 1987.
- [14] V.A. Gordin, et al., *Mathematical Problems and Methods in Hydrodynamical Weather Forecasting*, Gordon & Breach Publication House, Amsterdam et al, 2000.
- [15] A. Arnold, M. Ehrhardt, I. Sofronov, Approximation and fast calculation of non-local boundary conditions for the time-dependent Schrödinger equation, in: *Domain Decomposition Methods in Science and Engineering*, Springer, 2005, pp. 141–148.
- [16] V.A. Gordin, *Mathematics, Computer, Weather Forecasting and Other Scenarios of Mathematical Physics (in Russian)*, M.: Physmatlit, 2010, 2013.
- [17] A. Arnold, M. Ehrhardt, I. Sofronov, Discrete transparent boundary conditions for the Schrödinger equation: fast calculation, approximation, and stability, *Commun. Math. Sci.* 1 (2003) 501–556.
- [18] V.A. Gordin, Projectors using in forecasting schemes, in: *Proceedings of the USSR Hydrometeorological Center (in Russian)*, 1978, pp. 79–96.
- [19] V.A. Gordin, B.K. Dolmatov, Upper boundary condition in the numerical prediction of meteorological parameters, *Sov. Meteorol. Hydrol.* 4 (9) (1979) 25–33.
- [20] V.A. Gordin, Boundary condition of waves full absorption, which go away from prognostic area for difference equations, in: *Proceedings of the USSR Hydrometeorological Center (in Russian)*, 1982, pp. 104–120.
- [21] V.A. Gordin, The application of Padé vectorial approximation to the numerical solution of evolutionary forecasting equations, *Sov. Meteorol. Hydrol.* 7 (11) (1982) 24–37.
- [22] V.A. Gordin, *Mathematical Problems of the Hydrodynamical Weather Forecasting. Numerical Aspects (in Russian)*, Gidrometeoizdat, Leningrad, USSR, 1987.
- [23] A. Sommerfeld, Die greensche funktion der schwingungsgleichung, *J.-Ber. Deutsch Math.-Verein* 21 (1912) 309–353.
- [24] G.S. Morawetz, The limiting amplitude principle for arbitrary finite bodies, *Commun. Pure Appl. Math.* 18 (1965) 183–189.
- [25] I. Orlandi, A simple boundary condition for unbounded hyperbolic flows, *J. Comput. Phys.* 21 (1976) 251–269.
- [26] A.F. Bennett, Open boundary conditions for dispersive waves, *J. Atmos. Sci.* 33 (1976) 176–182.
- [27] A. Bayliss, E. Turkel, Radiation boundary conditions for wave-like equations, *Commun. Pure Appl. Math.* 33 (1980) 707–725.
- [28] M. Israeli, S.A. Orszag, Approximation of radiation boundary conditions, *J. Comput. Phys.* 41 (1981) 115–135.
- [29] J.B. Keller, D. Givoli, Exact non-reflecting boundary conditions, *J. Comput. Phys.* 82 (1989) 172–192.
- [30] S.V. Tsynkov, Numerical solution of problems on unbounded domains. a review, *Appl. Numer. Math.* 27 (1998) 465–532. Special Issue on Absorbing Boundary Conditions
- [31] T. Hagstrom, Radiation boundary conditions for the numerical simulation of waves, *Acta Numerica* 8 (1999) 47–106.
- [32] I. Gel'fand, G. Shilov, Chapter III - correctness classes for the cauchy problem, in: *Theory of Differential Equations*, Academic Press, 1967, pp. 105–164.
- [33] V.S. Ryaben'kii, Faithful transfer of difference boundary conditions, *Funct. Anal. Appl.* 24 (1990) 251–253.
- [34] V.S. Ryaben'kii, S.V. Tsynkov, *The Artificial Boundary Conditions for Numerical Solution of the External Viscous Flow Problems. I, II. Preprints (in Russian)*, M.: Inst. Appl. Mat., Russian Academy of Science, 1993, no 45, no 46
- [35] V.S. Ryaben'kii, S.V. Tsynkov, Artificial boundary conditions for the numerical solution of external viscous flow problems, *SIAM J. Numer. Anal.* 32 (1995) 1355–1389.
- [36] V.S. Ryaben'kii, S.V. Tsynkov, *A Theoretical Introduction to Numerical Analysis*, Chapman and Hall/CRC, 2006.

- [37] R.M. Feshchenko, A.V. Popov, Exact transparent boundary condition for the three-dimensional Schrödinger equation in a rectangular cuboid computational domain, *Phys. Rev. E* 88 (2013) 053308.
- [38] I.A. Zaitsev, I.L. Sofronov, Use of transparent boundary conditions for solution of two-dimensional elastodynamics problems with Azimuthal anisotropy, *Matem. Mod.* 19 (2007) 49–54.
- [39] M.F. Atiyah, R. Bott, L. Gårding, Lacunas for hyperbolic differential operators with constant coefficients. I, *Acta Math.* 124 (1970) 109–189.
- [40] A.O. Gelfond, *Calculus of Finite Differences*, Hindustan Publisher Corporation, 1971.
- [41] G.A. Baker Jr, P. Graves-Morris, Padé approximants. *Encyclopedia of Mathematics and its Applications*, volume 59, Cambridge University Press, 1996, 2009.
- [42] J. Nuttall, Asymptotics of diagonal Hermite – Padé polynomials, *J. Approx. Theory* 42 (1984) 299–386.
- [43] G.I. Barenblatt, *Scaling, Self-Similarity, and Intermediate Asymptotics: Dimensional Analysis and Intermediate Asymptotics*, volume 14, Cambridge University Press, 1996.
- [44] I.L. Sofronov, Conditions for complete transparency on a sphere for a three-dimensional wave equation, *Dokl. Akad. Nauk* 326 (1992) 953–957. (Russian)
- [45] I.L. Sofronov, About using transparent boundary conditions in aeroacoustics, *Matem. Mod.* 19 (2007) 105–112.
- [46] M. Abramowitz, I.A. Stegun, *Handbook of Mathematical Functions: With Formulas, Graphs, and Mathematical Tables*, Volume 55, Dover publications New York, 1972.
- [47] G. Szego, *Orthogonal Polynomials*, volume 23, American Mathematical Society, 1939.
- [48] F.W.J. Olver, *Introduction to Asymptotics and Special Functions*, Academic Press, New York and London, 1974.
- [49] S.L. Belousov, *Tables of Normalized Associated Legendre Polynomials*, Izd. Akad. Nauk USSR, 1956. In Russian
- [50] S.L. Belousov, Introduction, in: *Tables of Normalized Associated Legendre Polynomials*, Pergamon, 1962, pp. 3–15. volume 18 of *Mathematical Tables Series*
- [51] S.K. Lele, Compact finite difference schemes with spectral-like resolution, *J. Comput. Phys.* 103 (1992) 16–42.